Were transgressive black shales a negative feedback modulating glacioeustasy in the Early Palaeozoic Icehouse?

A. A. PAGE[1,2], J. A. ZALASIEWICZ[1], M. WILLIAMS[1] & L. E. POPOV[3]

[1]*Department of Geology, University of Leicester, Leicester, LE1 7RH, UK (e-mail: aap30@esc.cam.ac.uk)*

[2]*Department of Earth Sciences, University of Cambridge, Downing Street, Cambridge, CB2 3EQ, UK*

[3]*National Museum of Wales, Department of Geology, Cathays Park, Cardiff CF10 3NP, UK*

Abstract: The Early Palaeozoic Icehouse (Late Ordovician–Early Silurian, *c.* 455–425 Ma) was a remarkable event in the Earth's climatic history, marked by extensive glaciations occurring at a time of elevated atmospheric CO_2. The oceanography of the Early Palaeozoic Icehouse was markedly different from that of modern oceans, with frequent episodes of oceanic anoxia and high concentrations of CO_2 which may have acidified the oceans and restricted carbonate burial. Thus, the marine organic carbon reservoir may have more strongly influenced long-term changes in atmospheric CO_2 than at present. We suggest that deposition of black shales represented a major sink for atmospheric carbon. Sequence stratigraphy reveals that widespread black shale deposition occurred in transgressions, whereas regressions are characterized by deposition of bioturbated facies, allowing changes in lithofacies and deep-water redox conditions to be related to the Early Palaeozoic carbon cycle. Assuming increased temperature is a function of increased atmospheric CO_2, and that glacioeustatic sea-level can serve as a proxy for temperature due to changing ice volume, we infer that the deposition of transgressive black shales may have acted as a negative feedback mechanism, drawing down CO_2 and preventing the onset of runaway greenhouse conditions.

The Early Palaeozoic represents an important interval in Earth biosphere evolution. It post-dated the origin of large metazoans and complex, tiered marine food webs (Butterfield 1997), and is succeeded by the radiation of land plants (Berner 1998; Gensel & Edwards 2001). It therefore represents an intermediate state between the oxygen-poor Proterozoic palaeoenvironment and the well-oxygenated world of the Late Palaeozoic and post-Palaeozoic (Berner 2003; Catling & Claire 2005). This interval marks a non-actualistic solution to the Earth's carbon budget. Though generally considered an interval of long-lived, stable greenhouse conditions (e.g. Gibbs *et al.* 2000; Montañez 2002; Church & Coe 2003, fig. 5.4), major glaciations nonetheless occurred in the late Ordovician and early Silurian. These glaciations occurred at elevated atmospheric CO_2 (Royer 2006) and transitions between oxic and anoxic marine conditions were frequent (Figs 1d & 2). In a time before the evolution of a complex land biota, most of the organic carbon reservoir must have existed in oceans, where it was buried as black shale (Fig. 1). Despite recent advances in general circulation models (GCMs) and the application of climatically sensitive stable isotopes to infer palaeoenvironmental change, Early Palaeozoic climate remains somewhat enigmatic, no doubt in part due to its lack of analogue in the modern world.

Instead, the Early Palaeozoic needs to be understood in its own terms. Much as Charles Lapworth, Adam Sedgwick and Roderick Murchison carefully unpicked the undifferentiated 'greywacke' successions mapped by William Smith and Charles Lyell in the 19th century, and established the stratigraphic divisions of the Lower Palaeozoic (Rudwick 1985; Secord 1986; Oldroyd 1990), the 21st century sees the need for Early Palaeozoic workers to return to its stratigraphy and establish how global lithostratigraphic patterns of continental weathering and carbonate and black shale burial relate to its palaeoclimate, thereby determining the large-scale controls on the carbon cycle at this time.

The Early Palaeozoic carbon cycle and climate

Understanding chemical oceanography and carbon cycling in the Early Palaeozoic is difficult. The precise magnitude of atmospheric CO_2 at this time

From: WILLIAMS, M., HAYWOOD, A. M., GREGORY, F. J. & SCHMIDT, D. N. (eds) *Deep-Time Perspectives on Climate Change: Marrying the Signal from Computer Models and Biological Proxies.* The Micropalaeontological Society, Special Publications. The Geological Society, London, 123–156.
1747-602X/07/$15.00

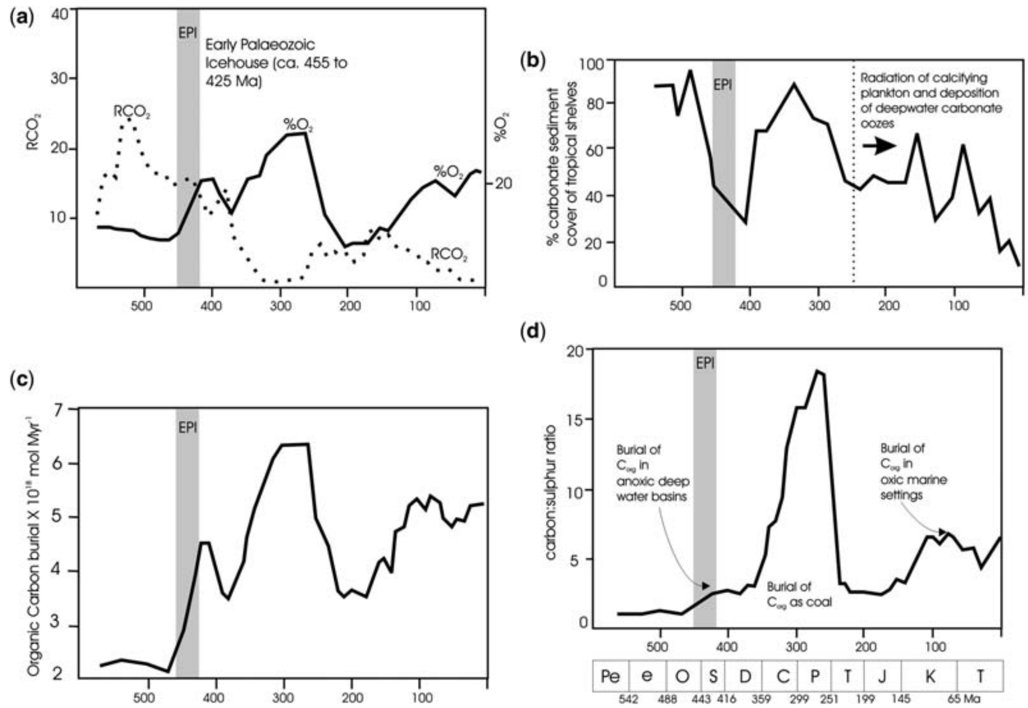

Fig. 1. Graphs illustrating changes in the nature of the carbon cycle through Phanerozoic time, showing the Early Palaeozoic dominated by organic-carbon burial in deep-marine anoxic waters under conditions of elevated atmospheric CO_2. (**a**) Temporal changes in atmospheric CO_2 relative to pre-industrial levels and partial pressure of atmospheric O_2 (after Berner 2001; Berner & Kothavala 2001). (**b**) Reduced carbonate deposition during the EPI as recorded in the relative proportion of low-latitude ($<30°$ N/S) shelf area occupied by carbonate sediments with time (data from Walker *et al.* 2002). (**c**) Temporal changes in organic carbon burial flux, showing a notable high in the EPI when organic carbon was predominantly buried in black shales (after Berner 2003). (**d**) Ratio of the accumulation rate of organic carbon and pyrite–sulphur (C/S) in sediments versus time (after Berner 2003): low C/S values reflect deposition of organic carbon in euxinic basins, high values correspond to burial in terrestrial freshwater swamps, and intermediate values are found in normal marine sediments (Berner & Raiswell 1983).

is uncertain, and the relation between CO_2 regulation and Early Palaeozoic climate is not fully resolved (see discussions in Ridgwell 2005; Royer 2006). However, available proxy data agree well with Berner and Kothavala's (2001) GEOCARB III model of atmospheric CO_2 levels over Phanerozoic time (Crowley & Berner 2001; Royer *et al.* 2004; Royer 2006), providing support for extremely elevated CO_2 levels in this interval (Fig. 1a). This provides support for key assumptions of the GEOCARB model and its descendants. Among these assumptions is that long-term drawdown of atmospheric CO_2 into the oceans was a consequence of (a) continental silicate weathering and burial in carbonates, and (b) photosynthesis and burial of organic carbon (Berner 1991, 1994, 2006; Berner & Kothavala 2001). CO_2 regulation must have been reflected in the specific pattern of organic and inorganic carbon burial in the Early Palaeozoic (Fig. 1), which differs notably from that of the Neoproterozoic (Rothman *et al.* 2003) and the rest of the Palaeozoic (Berner 2003).

In the Early Palaeozoic, carbonate burial was restricted to the continental shelves (Walker *et al.* 2002), whilst organic carbon was predominantly buried in deep-water anoxic environments (Fig. 1d). The advent of biomineralization in the Cambrian explosion facilitated carbonate burial relative to the Neoproterozoic (Rothman *et al.* 2003; Ridgwell 2005). However, the Early Palaeozoic may have lacked a well-developed marine carbonate buffer, which is highly sensitive to increased atmospheric CO_2 (Barker *et al.* 2003). The radiation of the calcifying plankton in the Triassic profoundly affected the pattern of marine carbonate deposition (Martin 1995), and a modern ocean analogue for carbonate burial may not be applicable before this (cf. Ridgwell 2005). Likewise, the advent of digestion, bioturbation and a macroplankton faecal express in the Cambrian explosion (Butterfield 1997) no doubt significantly affected the cycling of the organic carbon reservoir, which lacked the sustained, large-scale fluctuations witnessed in the Neoproterozoic (Hayes *et al.* 1999; Rothman *et al.* 2003). However, prior to the greening of the continents in the Late Palaeozoic (Berner 1998; Gensel & Edwards 2001), the marine organic carbon reservoir dominated the burial of organic carbon (Berner 2003), and the frequent intervals of marine anoxia that typify the Early Palaeozoic are probably a consequence of this (Figs 1d & 3).

Constraining CO_2 drawdown in this interval requires good estimates of the burial fluxes of carbonates and organic carbon (Fig. 1b, c). There are two ways of achieving such estimates. The first approach takes the known volume of carbon held in preserved strata and applies a correction to account for the progressive volume loss due to erosion, subduction and metamorphism (e.g. Berner & Canfield 1989; Walker *et al.* 2002). The second approach applies GCMs and/or geochemically appropriate mass-balance models to proxy and/or mass flux curves (e.g. Berner 2003; Locklair & Lermann 2005; Ridgwell 2005). Neither of these methods is without problems: the former depending heavily on the dataset and the latter depending on the assumptions of the model. Though sophisticated approaches such as GCMs or multifactor box modelling allow palaeoclimatic hypotheses to be quantitatively established and/or tested, they may be extremely sensitive to certain parameters and differing algorithms can produce different results based on similar datasets (see Haywood *et al.* 2005). Moreover, GCMs are highly dependent on changes in palaeogeography, ocean bathymetry, pCO_2, insolation and albedo. So, unless these factors are well constrained, their results should be considered conservatively before universally accepting their applicability in non-actualistic environments (cf. Ridgwell 2005).

The Early Palaeozoic climate includes the seemingly paradoxical occurrence of extensive glaciations (the Early Palaeozoic Icehouse or EPI as defined below) at elevated atmospheric CO_2 (Royer 2006). Given the long-recognized coupling of CO_2 and temperature (Arrhenius 1896; Chamberlin 1899) and more recent affirmations of the sensitivity of temperature to CO_2 (e.g. Shackleton 2000; Zachos *et al.* 2001; Kump 2002; Siegenthaler *et al.* 2005), a link between CO_2 and temperature in the Early Palaeozoic seems reasonable. Decreased cosmic ray flux also may have contributed to globally cooler temperatures during the EPI (Veizer *et al.* 2000; Shaviv 2002; Shaviv & Veizer 2003), but this was insufficient to induce glaciation alone (Royer 2006).

Most models suggest that atmospheric CO_2 was the key control on temperature and ice formation in the Ordovician and Silurian, predicting a pCO_2-ice threshold around 3000 ppm (Kump *et al.* 1999; Hermann *et al.* 2003, 2004*a*, *b*; Royer 2006). These values are significantly lower than the GEOCARB III or GEOCARBSULF estimate for Hirnantian CO_2 levels at *c.* 4000 ppm (Berner & Kothavala 2001; Berner 2006). The GEOCARB/GEOCARBSULF estimates are consistent with estimates from goethite (Yapp & Poths 1992) and significantly lower than the single palaeosol-based estimate of CO_2 for the Ashgill at *c.* 5600 ppm (Royer 2006). However, these models operate on longer timescales than the duration of the short-lived Hirnantian glacial maximum (cf. Sutcliffe *et al.* 2000), so the discrepancy between the estimated CO_2-ice threshold and estimates of atmospheric CO_2 may not be inconsistent (cf. Royer 2006). That is, glacial events could have been too rapid to be captured by either these models or the sparse proxy record. Individual glaciations in the EPI may have been short-lived events related to rapid CO_2 drawdown and cooling (e.g. Kump *et al.* 1999).

A stratigraphic approach to Early Palaeozoic glaciations

Lithostratigraphic correlation may establish a link between deposition of CO_2 sinks and glaciations during the Early Palaeozoic. CO_2 may be drawn down from the atmosphere and sequestered in rocks by (a) photosynthesis and burial of organic carbon, or (b) continental silicate weathering and carbonate deposition. In glacial intervals, changes in ice-volume allow changes in glacioeustatic sea-level to serve as a proxy for atmospheric CO_2 (assuming that ice volume was a decreasing function of temperature and that temperature was an increasing function of atmospheric CO_2). The stratigraphic occurrence of carbonates and argillaceous sediments has been well documented in the identification of Primo/Secundo or Humid/Arid episodes (e.g. Jeppsson 1990, 1997; Aldridge *et al.* 1993; Jeppsson *et al.* 1995; Bickert *et al.* 1997; Cramer & Saltzman 2007; see also discussion). We adopt a complementary approach by comparing the stratigraphic distributions of black shale with glacioeustatic sea-level curves, isotopic data and evidence of glaciations.

This approach depends on the selection of high quality datasets with well-resolved stratigraphies and accurate correlations. These are discussed in the Appendix. We have been cautious in assigning evidence of ice formation to the glacial maxima, as discussed below.

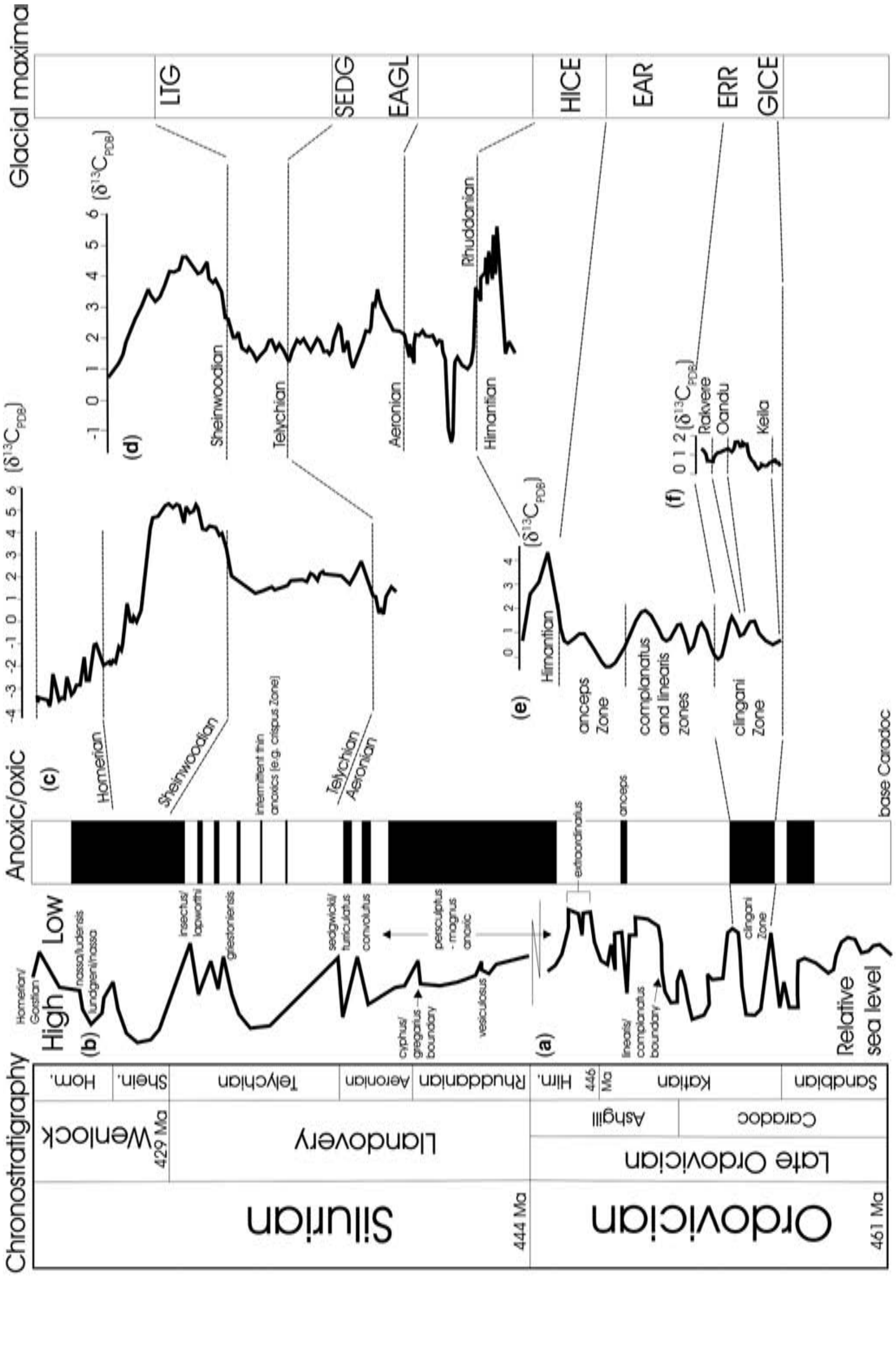

Chronostratigraphy
Silurian
Ordovician
444 Ma
461 Ma
Wenlock
429 Ma
Llandovery
Late Ordovician
Ashgill
Caradoc
Hom.
Shein.
Telychian
Aeronian
Rhuddanian
Hirn.
446 Ma
Katian
Sandbian
High
Low
Relative sea level
(a)
(b)
Anoxic/oxic
(c)
Homerian
Sheinwoodian
Telychian
Aeronian
base Caradoc
(d)
(e)
(f)
Himantian
anceps Zone
complanatus and linearis zones
clingani Zone
Rhuddanian
Rakvere
Oandu
Keila
Glacial maxima
LTG
SEDG
EAGL
HICE
EAR
ERR
GICE

The Early Palaeozoic Icehouse

The Early Palaeozoic Icehouse (EPI) was an approximately 30-million-year interval comprising seven currently recognized glacial maxima (Table 1; Fig. 2). We propose that the EPI began with the Guttenberg Limestone carbon isotope excursion (GICE) in the Caradoc (Ordovician), and ended with Ireviken event deglacial transgression of the earliest Wenlock (Silurian). The EPI reached its greatest extent in the short-lived Hirnantian event identified by Brenchley *et al.* (1994), but there is a good evidence for extensive ice formation and significant glacioeustatic change throughout the EPI (Tables 1 & 2; Fig. 2). Several other authors have argued for an extended period of glaciation (e.g. Frakes *et al.* 1992; Eyles 1993; Evans 2003; Ghienne 2003; Kaljo *et al.* 2003; Nielsen 2003*a*; Saltzman & Young 2005).

The sedimentary record of glaciations in the EPI is predominantly held on Gondwana, with Ordovician deposits generally found in Africa, and Silurian deposits in South America (Table 2; Eyles 1993; Díaz-Martínez & Grahn 2007). This continental-scale diachronism may reflect the movement of Gondwana across the South Pole (cf. Fortey & Cocks 2003). The Tamadjert Fm of Saharan Africa displays a 200 m sequence of glacial deposits. These include extensive tillites and diamictites and abundant evidence of glacial erosion stretching from the Caradoc to the late Llandovery or even the earliest Wenlock (Beuf *et al.* 1971; Biju-Dival *et al.* 1981 and references therein). Three periods of continent-wide diamictite deposition are recognized in the early Silurian of South America (Caputo 1998; Díaz-Martínez 2007). After the latest Llandovery, the South American record of glaciation becomes ambiguous. Glaciogenic diamictites in the San Gabán–Cancañiri–Zapla and Nhamundá Fms (Table 2) are overlain by strata yielding early Wenlock conodonts and late Telychian–early Wenlock chitinozoans respectively (Díaz-Martínez 2007; Grahn in Cramer & Saltzman 2007). The most recent works on these glacial deposits consider them as having an entirely Llandovery age (Díaz-Martínez 2007; Díaz-Martínez & Grahn 2007). Though the Kirusillas Fm of Bolivia contains diamictites of early Wenlock age (Merino 1991; Díaz-Martínez 2007), these lack glacially abraded clasts and are considered to be sediment gravity flows (Díaz-Martínez 2007; Díaz-Martínez & Grahn 2007).

The coupled, rapid variation in the isotopic and glacioeustatic records (Fig. 2) that continues throughout the EPI clearly marks a genetic change in the Earth system. The strong co-variation in these records may arise from the interval being a prolonged icehouse event (Kaljo *et al.* 2003; Nielsen 2003*b*). The good correspondence of third-order variation in eustatic sea-level curves (Ross & Ross 1996; Nielsen 2003*a*, *b*), along with evidence of ice advance and retreat (Table 2) argues for ice-volume controlling sea-level during the EPI. Likewise, there is strong co-variation in $\delta^{13}C$ and $\delta^{18}O$ data throughout the EPI (cf. Azmy *et al.* 1998; Shields *et al.* 2003). During the EPI, we interpret positive $\delta^{13}C$ excursions as being due to increased weathering of shallow carbonates exposed in regressions (cf. Kump *et al.* 1999; Melchin & Holmden 2006; see also the Appendix). Whilst in the EPI, positive $\delta^{18}O$ excursions are interpreted as due to cooling rather than increased salinity alone (Azmy *et al.* 1998). Therefore, coupled, positive $\delta^{13}C$ and $\delta^{18}O$ excursions may indicate glaciations if consistent with other evidence.

The synchronous onset of significant, coupled isotopic and eustatic fluctuations at the onset of the Katian in the Ordovician, mark the beginning of the EPI (Fig. 2; Patzkowsky *et al.* 1997; Kaljo *et al.* 2003; Nielsen 2003*a*, *b*). This corresponds to the mid-Caradoc *clingani* graptolite Zone (Cooper & Sadler 2004; Goldman *et al.* 2005). There is, though, also evidence of glacial erosion and a regression in the earliest Caradoc (Hamoumi 1999; Nielsen 2003*a*, *b*). The termination of the EPI is marked by the decoupling of isotopic and glacioeustatic variation in the earliest Wenlock (Fig. 2). In the latest Telychian, there is good evidence of ice (Table 2). Prior to the early

Fig. 2. (Opposite) The relationship between extent of marine anoxia and sea-level during the EPI based on the chronostratigraphy of Cooper & Sadler (2004) and Melchin *et al.* (2004), but placing the Llandovery–Wenlock Boundary at Ireviken datum 2 after the recommendations of Loydell *et al.* (2003) and Calner *et al.* (2004). Transgressive anoxia is apparent by comparing (**a**) summary sea-level curves to (**b**) the oxic/anoxic stratigraphy (dark bands, anoxic; white, oxic). Sea-level curves drawn after Ross & Ross (1996) and Nielsen (2003*a*); the oxic/anoxic stratigraphy is compiled from Figure 3. The Ross & Ross (1996) curve has been modified in accordance with its recorrelation in Loydell (1998). (**c**–**f**) Stable carbon-isotope curves: (c, d) redrawn from Kaljo *et al.* (2003); (e) redrawn from Kaljo *et al.* (2004); (f) redrawn from Ainsaar *et al.* (1999). (**g**) Glacial maxima recognized in Table 1: GICE, Guttenberg regression; ERR, early Rakvere regression; EAR, early Ashgill regression; HICE, Hirnantian glaciation; EAGL, early Aeronian glaciation; SEDG, sedgwickii Zone glaciation; LTG, late Telychian glaciation.

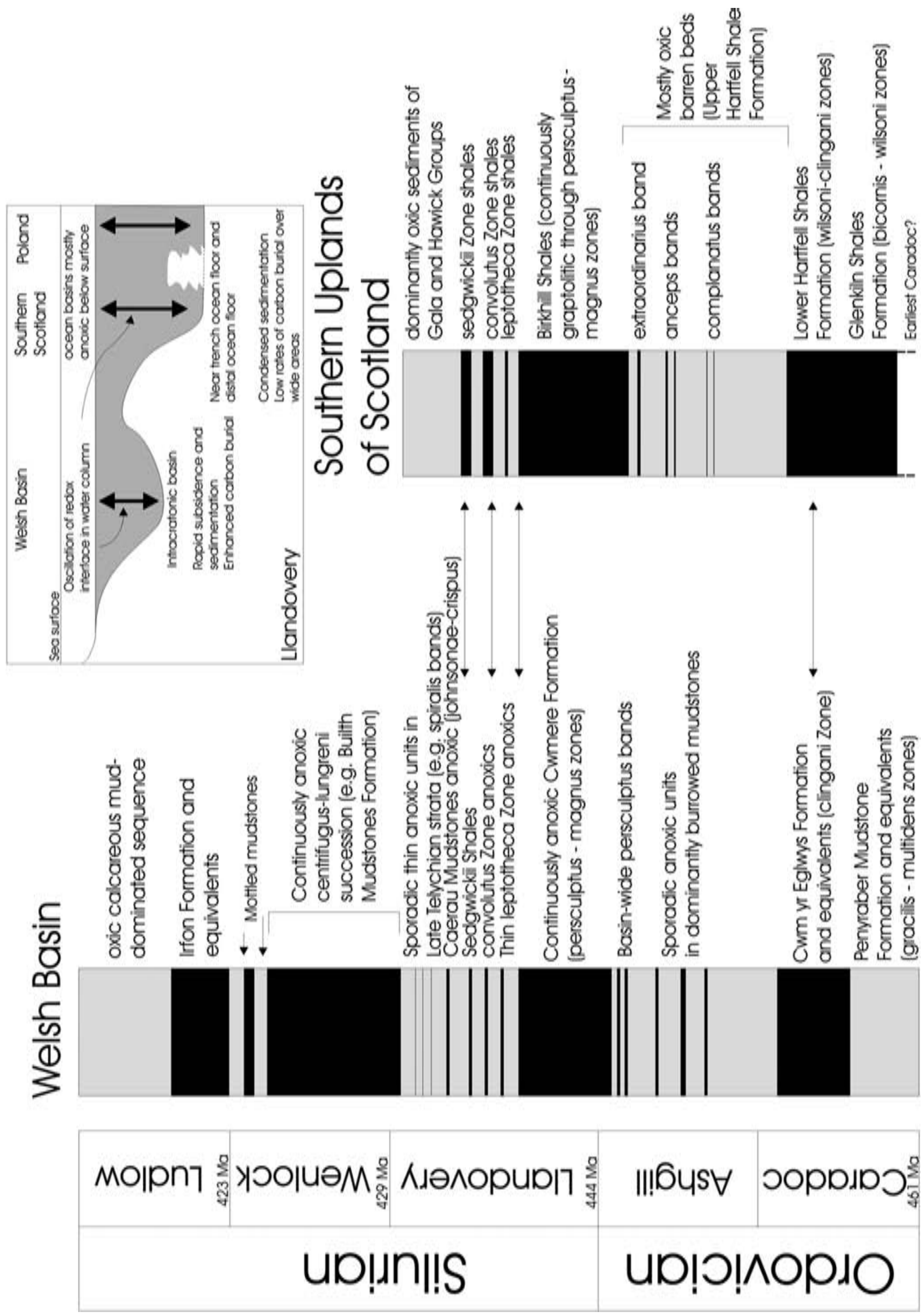
Sea surface
Welsh Basin
Southern Scotland
Poland
Oscillation of redox interface in water column
ocean basins mostly anoxic below surface
Intracratonic basin
Rapid subsidence and sedimentation
Enhanced carbon burial
Near trench ocean floor and distal ocean floor
Condensed sedimentation
Low rates of carbon burial over wide areas
Llandovery
Welsh Basin
Southern Uplands of Scotland
Silurian
Ordovician
Ludlow
423 Ma
Wenlock
429 Ma
Llandovery
444 Ma
Ashgill
Caradoc
461 Ma
oxic calcareous mud-dominated sequence
Irfon Formation and equivalents
Mottled mudstones
Continuously anoxic centrifugus-lungreni succession (e.g. Builth Mudstones Formation)
Sporadic thin anoxic units in
Late Telychian strata (e.g. spiralis bands)
Caerau Mudstones anoxic (johnsonae-crispus)
Sedgwickii Shales
convolutus Zone anoxics
Thin leptotheca Zone anoxics
Continuously anoxic Cwmere Formation (persculptus - magnus zones)
Basin-wide persculptus bands
Sporadic anoxic units in dominantly burrowed mudstones
Cwm yr Eglwys Formation and equivalents (clingani Zone)
Penyraber Mudstone Formation and equivalents (gracilis - multidens zones)
dominantly oxic sediments of Gala and Hawick Groups
sedgwickii Zone shales
convolutus Zone shales
leptotheca Zone shales
Birkhill Shales (continuously graptolitic through persculptus - magnus zones)
extraordinarius band
anceps bands
complanatus bands
Mostly oxic barren beds (Upper Hartfell Shale Formation)
Lower Hartfell Shales Formation (wilsoni-clingani zones)
Glenkiln Shales Formation (bicornis - wilsoni zones)
Earliest Caradoc?

Wenlock Ireviken excursion *sensu* Cramer & Saltzman (2005, 2007), there are coupled, positive excursions in $\delta^{13}C$ and $\delta^{18}O$ (Bickert *et al.* 1997; Azmy *et al.* 1998) during a regression (cf. Loydell 1998). The Ireviken excursion itself occurred at a time of climatic amelioration (Cramer & Saltzman 2005, 2007). It witnessed a positive $\delta^{13}C$ excursion at globally high sea-level (Cramer & Saltzman 2005, 2007). This positive $\delta^{13}C$ excursion was accompanied by a slight negative $\delta^{18}O$ excursion, which may indicate warming (Bickert *et al.* 1997; Azmy *et al.* 1998). The decoupling of isotopic and glacioeustatic co-variation in the early Wenlock (Fig. 2) marks a genetic change in the Earth system. It is unlike any interval in the EPI itself, and accompanied climatic amelioration witnessed in the development of extensive limestone reefs (e.g. Copper 1994; Brunton *et al.* 1998).

Most recent work on Early Palaeozoic glaciations has focused on the Hirnantian (e.g. Sutcliffe *et al.* 2001; Hermann *et al.* 2004*a*, *b*; Armstrong *et al.* 2005; Le Heron *et al.* 2005) since Brenchley *et al.* (1994) argued for a short-lived Late Ordovician glaciation. This may partly reflect its coincidence with a mass extinction at a major stratigraphic division (e.g. Chen *et al.* 2000, 2005), as well as the deposition of major hydrocarbon source rocks in overlying strata (Lüning *et al.* 2000; Berner 2003). However, we have used the criteria of Brenchley *et al.* (1994) to recognize six more glacial maxima in the EPI. Namely, that sequence stratigraphic evidence for large, global lowstands, coincident with positive $\delta^{13}C$ and $\delta^{18}O$ excursions and evidence of ice formation, indicates a glacial maximum (Table 1; Fig. 2).

Within the EPI, individual glacial maxima were separated by warmer intervals (e.g. Fortey & Cocks 2005), and recent research has highlighted clear variability in the Silurian palaeoenvironment (e.g. Jeppsson 1990; Aldridge *et al.* 1993; Bickert *et al.* 1997; Johnson 2006; Calner & Eriksson 2006). The frequent evidence of ice formation and rapid, third-order variation in eustatic sea-level (e.g. Azmy *et al.* 1998; Caputo 1998; Loydell 1998; Hamoumi 1999; Ghienne 2003; Nielsen 2003*a*, *b*; Johnson 2006) suggests that ice-sheets may have dynamically expanded and retreated during the EPI.

Glacial maxima in the EPI

The seven glacial maxima of the EPI have been either assigned to existing named events or given stratigraphically descriptive names based on their nature. Thus, some are referred to as regressions and others are called glaciations, depending on the weight of evidence. We deal with each glacial maximum in turn below.

The Guttenberg regression (*GICE*) as defined in Table 1 and Figure 2 is named after the Guttenberg Limestone Member of the Decorah Fm in the Upper Mississippi Valley, USA, where the positive $\delta^{13}C$ excursion was first recognized (Hatch *et al.* 1987). This carbon isotope excursion has subsequently been recognized elsewhere and is considered to represent a global event (e.g. Patzkowsky *et al.* 1997; Ainsaar *et al.* 1999; Kaljo *et al.* 2004). It was accompanied by a synchronous positive $\delta^{18}O$ excursion of earliest *clingani* graptolite Zone age (Shields *et al.* 2003; Tobin *et al.* 2005). The high-resolution chemostratigraphy of Ludvigson *et al.* (2004) shows that the GICE occurred after three other smaller positive $\delta^{13}C$ excursions, and that it took place in the *P. tenuis* conodont Zone and *americanus* graptolite Zone (equivalent to the earliest *clingani* Zone). In the Katian GSSP (Black Knob Ridge, Oklahoma, USA), there is a seemingly synchronous $\delta^{13}C$ excursion just above the Sandbian–Katian boundary (Goldman *et al.* 2005). This is coincident with the late Keila age regression noted by Kaljo *et al.* (2003) and Nielsen (2003*a*); and Ludvigson *et al.* (2004) also noted that the GICE occurred in a time of stratigraphical downlap. Due to the lack of well-dated glacial deposits in this interval (Table 2), there is no unambiguous link with ice formation, but it may represent a period of cooling as continental ice-sheets were beginning to expand (cf. Patzkowsky *et al.* 1997).

The early Rakvere regression (*ERR*) is named after the stage in Estonia, where it is recognized in the carbon isotope and sequence stratigraphic records (Table 1; Fig. 2). This regression took place within the latest *clingani* graptolite Zone (Nielsen 2003*a*), equivalent to the *A. superbus* conodont Zone (Nõlvak *et al.* 2006). Though there is evidence for glacial erosion at this time (Table 2), there is no evidence for extensive tillite formation.

Fig. 3. (Opposite) Correlation of marine anoxia between UK depositional basins based on the widespread occurrence of graptolite-bearing anoxic mudrock facies, with inset schematic showing the differing depositional environments associated with this facies. Stratigraphies and inset compiled from original work of Toghill (1968); Cave (1979); Baker (1981); White *et al.* (1991). Davies *et al.* (1997, 2003); Pratt *et al.* (1995); Zalasiewicz *et al.* (1995); Porębska & Sawłowicz (1997); Schofield *et al.* (2004); and Verniers & Vandenbroucke (2006). Note that the Hirnantian and Llandovery oxic–anoxic stratigraphy of the Welsh Basin bears close resemblance to the Lake District and Howgill Fells succession of Northern England (Rickards 1970; Hutt 1974; Rickards & Woodcock 2005).

Table 1. *Name, age and evidence for each of the seven glacial maxima in the EPI;* $\delta^{13}C_{PDB}$ *= most positive value of carbon isotopes in positive excursion based on regional isotopic compilations;* $\Delta\delta^{13}C_{PDB}$ *= total change in carbon isotope values during positive isotope excursions based on regional isotopic compilations;* $\delta^{18}O_{PDB}$ *= most positive value of oxygen isotopes in positive excursion recorded in brachiopod shells;* $\Delta\delta^{18}O_{PDB}$ *= total change in oxygen isotope values during positive isotope excursions recorded in brachiopod shells; oxygen isotope data taken from Tobin* et al. *(2005) for the Guttenberg regression, from Brenchley* et al. *(1994) for the Hirnantian Glaciation in the Baltic region, and from Azmy* et al. *(1998) for all Silurian events; all other data compiled from Table 2, Figure 2, Kaljo* et al. *(2007), and references therein*

Glacial maxima	Evidence for ice	$\Delta\delta^{13}C_{PDB}$	$\delta^{13}C_{PDB}$	$\Delta\delta^{18}O_{PDB}$	$\delta^{18}O_{PDB}$	Extent of regression	Timing
Guttenberg regression	poorly dated glacial-erosive features in North Africa	~ + 1.0‰	+1.7‰	~ + 2.3‰	−2.7‰	medium	early *caudatus* graptolite Zone
early Rakvere regression	poorly dated glacial-erosive features in North Africa	~ + 0.8‰	+1.8‰	–	–	medium	late *clingani* graptolite Zone
early Ashgill regression	poorly dated Ashgill tillites and glacial erosive features in North Africa	~ + 1.2‰	+2.0‰	–	–	large	end *linearis* graptolite Zone
Hirnantian glaciation	Pan-Gondwanan tillites & diamictites containing Hirnantia fauna	~ + 4.0‰	+4.3‰	~ + 4.2‰	0‰	large	*extraordinarius*–early *persculptus* graptolite Zones
early Aeronian glaciation	*gregarius* Zone diamictite in South America	~ + 2.0‰	+3.0‰	~ + 0.6‰	−4.5‰	small	*gregarius* (?*magnus*) graptolite Zone
sedgwickii s.l. glaciation	well-dated diamictites in South America	~ + 0.5‰	+2.0‰	~ + 0.7‰	−4.4‰	medium	*sedgwickii* graptolite Zone
late Telychian glaciation	well-dated diamictites in South America	~ + 1.5‰*	+2‰*	~ + 1.0‰*	−4.6‰*	large	?*insectus*–*lapworthi* graptolite Zones

*These excursions occur in the late Telychian significantly preceding the Ireviken excursion *sensu* Cramer & Saltzman (2005, 2007).

This, along with its expression in the sea-level and isotopic record, may indicate that it was a relatively small, short-lived event.

The early Ashgill regression (*EAR*) appears to be a more significant event based on both its sea-level and isotopic record (Table 1; Fig. 2). Nielsen (2003*a*) noted significant regression in the early Ashgill *complanatus* graptolite Zone. This is synchronous with regression and a positive $\delta^{13}C$ excursion noted by Kaljo *et al.* (2004) at the basal Pirgu stage in Estonia (Nõlvak *et al.* 2006). There is good evidence for glacial sediments being deposited in the Ashgill of North Africa (which was close to the palaeomagnetic South Pole). However, this regression cannot be tied to any one particular high-latitude event, due to imprecision in the biostratigraphy of these successions (Table 2).

The Hirnantian glaciation (*HICE*) occurs as two pulses of glaciation within the *extraordinarius–persculptus* graptolite Zones (Sutcliffe *et al.* 2000). It represents the glacial maximum of the EPI and has received extensive study. It is well constrained and clearly globally extensive. The extent of the eustatic and isotopic variations associated with this are shown in Table 1 and Figure 2, with more detailed treatment of this event being found in Brenchley *et al.* (1994, 2003), Marshall *et al.* (1997), Sutcliffe *et al.* (2001), and Armstrong (this volume).

The early Aeronian glaciation (*EAGL*) has a significant expression in marine carbon isotope values, but this may also represent an increased effect of carbonate weathering relative to the Ordovician glaciations. There is clear evidence for ice formation during the *gregarius* graptolite Zone (Tables 1 & 2), but this is a long interval, which can be subdivided into the *triangulatus*, *magnus* and *argenteus* zones (see Hutt 1974). Precisely how ice formation in this event correlates with sea-level is unclear: the Rhuddanian–Aeronian boundary regression seen in the Ross & Ross (1996) sea-level curve is not recognized in other records, which show marked regressions at or around the *magnus–argenteus* graptolite Zone boundary (Johnson *et al.* 1991; Loydell 1998; Johnson 2006). Azmy *et al.* (1998) show the onset of a positive $\delta^{13}C$ and $\delta^{18}O$ excursion in the *triangulatus* Zone, but do not present data for the *magnus* and *argenteus* zones. Kaljo *et al.* (2003) illustrate a longer $\delta^{13}C$ excursion, which both they and Johnson (2006) correlate to an early Aeronian glaciation.

The sedgwickii *graptolite Zone glaciation* (*SEDG*) is discussed at length below. Loydell (1998) and Johnson (2006) both show major regressions at this time. Azmy *et al.* (1998) and Johnson (2006) argued for glaciations based on isotopic data, which we note correspond to well-dated diamictites (Table 2).

The late Telychian glaciation (*LTG*) is the final glacial maximum of the EPI. As noted above, the final pulse of diamictite deposition in South America can be assigned to the late Telychian, though cannot be constrained to any particular zone (Table 2). The late Telychian is coincident with regressions: Figure 2 illustrates a rapid sea-level fall in the late *insectus* graptolite Zone (see also Appendix), while Loydell (1998) shows a rapid regression in the *lapworthi* graptolite Zone with a lowstand throughout the *lapworthi–insectus* interval, also recognized in SW Siberia by Yolkin *et al.* (1997). During this interval, Azmy *et al.* (1998) show a positive $\delta^{13}C$ and $\delta^{18}O$ excursion, beginning in the *crenulata* graptolite Zone and reaching a maximum in the *centrifugus* graptolite Zone. Likewise, Kaljo *et al.* (1998, 2003) show that the onset of this positive $\delta^{13}C$ transition occurred in the late Llandovery, with subsequent studies placing this in the *Pt. amorphognathoides* conodont Zone in Estonia (Kaljo & Martma 2006) and possibly towards its base (see Cramer & Saltzman 2005). As such, we suggest this glaciation occurred within the *lapworthi–insectus* graptolite Zone interval.

Oxic–anoxic stratigraphy and sea-level in the EPI

Correlating the UK oxic–anoxic stratigraphy against glacioeustatic sea-level curves reveals a repeated relation between black shale deposition and deglacial transgressions throughout the EPI (Figs 2 and 3). Conversely, glaciations themselves correspond to well-oxygenated deep waters. Comparison with deep-water successions influenced by the Rheic and Palaeotethys oceans suggests these oxic–anoxic transitions may have had global extent. The glacioeustatic sea-level and oxic–anoxic stratigraphy are discussed briefly below, before the post-Hirnantian transgression and *sedgwickii* Zone regressions are dealt with in detail.

All the oxic to anoxic transitions of the EPI represent maximum flooding surface transgressive black shales (*sensu* Wignall & Maynard 1993; Wignall 1994). They are regionally extensive and post-date glacial maxima (Fig. 2; Woodcock *et al.* 1996; Armstrong *et al.* 2005). The GICE regression precedes the development of extensive anoxia within the Welsh Basin during the *clingani* graptolite Zone. At this time, widespread, organic carbon-rich and phosphatic black shales, such as the Nod Glas and Cwm-yr-Eglwys Mudstone Fms (Cave & Dixon 1993; Davies *et al.* 2003), were laid down upon oxic mudrocks and limestones, such as the Carswyn and Penyraber Mudstone Fms (Fig. 2; Pratt *et al.* 1995; Davies *et al.* 2003). In the

Platteville–Decorah formations of eastern Iowa (USA), the Guttenberg Member is brown shale (Ludvigson *et al.* 2004). This occurs above a well-laminated shale and widespread phosphatic bed of the Spects Ferry Member and below the well-laminated shales and blackened/phosphatic hardgrounds of the Ion Member (Ludvigson *et al.* 2004). Likewise, pyritic graptolite shales of *clingani* Zone age Nakkholmen Fm in the Oslo area (Norway) overlie limestones, as do coeval graptolite shales in the lower Mossen Fm of Västergötland (Nielsen 2003*a*). This represents an oxic–anoxic transition that reflects a profound drowning event (Nielsen 2003*a*, *b*).

The early Ashgill regression preceded the *anceps* graptolite Zone transgression, with the UK record witnessing simultaneous intervals of black shale deposition in an otherwise oxic succession (Fig. 3). For example, the 'Red Vein' in Wales, a thin unit of anoxic mudstones bearing graptolites of probable *anceps* graptolite Zone age (e.g. Schofield *et al.* 2004), appears synchronous with the *anceps* bands in Scotland (Williams 1982). The Hirnantian glaciation, with an acme in the *extraordinarius* graptolite Zone (Sutcliffe *et al.* 2000), preceded the deposition of globally extensive transgressive black shales in the *persculptus*–*acuminatus* graptolite zones (Fig. 4 & text below). Likewise, the *sedgwickii* graptolite Zone glacial event is characterized by the deposition of oxic facies during a lowstand, which is sandwiched between transgressive black shales (Fig. 5 & text below). The *convolutus* graptolite Zone represents a major transgression and global highstand following the early Aeronian glaciation, with widespread black shale deposition noted in Loydell (1998), synchronous with the UK *convolutus* bands of graptolitic shale (Fig. 3). Similarly, the deglacial transgression in the latest Telychian is characterized by the onset of anoxia and the deposition of marine black shales in the *centrifugus* Zone in the UK. These include the Builth Mudstones in the Welsh Basin (Woodcock *et al.* 1996; Zalasiewicz & Williams 1999) and the Brathay Mudstones in northern England (Rickards 1970; Rickards & Woodcock 2005). These were both deposited on essentially oxic, late Llandovery successions (Davies *et al.* 1997; Rickards & Woodcock 2005). In Baltoscandia, this event also sees the deposition of graptolitic shales on greenish-grey marlstones in the Ohesaare core from Estonia (Loydell *et al.* 1998) and on oolitic limestone/grey-green shale interbeds in Bornholm (Bjerreskov 1975; AAP unpublished observations April 2006). Similarly, Lüning *et al.* (2005) noted the deposition of 'hot shales' on the North African/Arabian margin during the *centrifugus* to *firmus* graptolite zones. The relation between deglaciation, transgression and anoxia in the late Telychian–early Wenlock has been reviewed in depth by Cramer and Saltzman (2007). Further examples of transgressive black shales deposited after the Llandovery glaciations may be found in Loydell (1998).

During the EPI, the deposition of bioturbated facies, representing conditions of deep-marine oxygenation, occurred during regressions and glacial maxima (Brenchley 1988; Loydell 1998; Fig. 2). The Hirnantian and *sedgwickii* Zone glacial maxima correspond to intervals of grey shale and deposition of mottled (i.e. bioturbated) mudstones (Figs 4 & 5). Likewise, the positive carbon isotope excursion in the mid-*gregarius* graptolite Zone that marks the early Aeronian glaciation may correspond to the onset of oxic deposition in the mid-*magnus* graptolite Zone of the Welsh Basin (Fig. 3). In Black Knob Ridge, Oklahoma, the maximum $\delta^{13}C$ excursion corresponding to GICE occurs in an interval with extremely diminished C_{org} content in an otherwise organic-rich sequence (Goldman *et al.* 2005). This perhaps represents an interval of increased deep-water ventilation (cf. Ludvigson *et al.* 2004). The early Rakvere regression (latest *clingani* graptolite Zone) may possibly correlate with the transition from black shales to limestone at Whitland, South Wales. Also, the Fjäcka Shales of Sweden are deposited on the well-oxygenated facies of the Slandrom Limestone of Sweden and Bestorp Limestone of Västergötland, representing transgressive black shales deposited after the early Rakvere event (Männil & Meidla 1994).

Transgressive anoxia: post-Hirnantian glaciation oceanic anoxic event

The late *persculptus* and *acuminatus* graptolite Zones are characterized by deposition of globally extensive transgressive black shales (Fig. 4) immediately following the *extraordinarius*–early *persculptus* graptolite Zone acme of the Hirnantian glaciation (Sutcliffe *et al.* 2000, 2001), suggesting a fundamentally deglacial origin for the onset of global marine anoxia. This followed the enhanced deep ocean circulation and oxygenation that characterized the Hirnantian glaciation (Brenchley 1988; Brenchley *et al.* 1994; Armstrong & Coe 1997). High-palaeolatitude sedimentary successions typically consist of Hirnantian glacial deposits immediately overlain by black shales (e.g. Sutcliffe *et al.* 2001; Armstrong *et al.* 2005, 2006). Low-palaeolatitude settings see unambiguously oxic facies such as deep-water bioturbated mudstones overlain by deglacial black shales (e.g. Mu 1988; Armstrong & Coe 1997; Davies *et al.* 1997; Chen *et al.* 2000, 2005; Verniers &

Vandenbroucke 2006). Shallow-water shelly faunas in low- to mid-palaeolatitudes may also be buried below *persculptus* graptolite Zone black shales (e.g. Bjerreskov 1975; Mu 1988; Davies *et al.* 1997; Chen *et al.* 2000, 2005), though some shallow successions in the palaeotropics may see limestone deposition going on uninterrupted (e.g. Barnes & Bolton 1988). These deglacial black shales are widely palaeogeographically distributed and represent a global event (Fig. 4) perhaps comparable to the Mesozoic oceanic anoxic events (cf. Cohen *et al.* 2004).

Deposition of regionally extensive black shales on maximum flooding surfaces (*sensu* Wignall & Maynard 1993; Wignall 1994) in the *persculptus* graptolite Zone provides strong evidence for their onset in the end Ordovician–early Silurian transgression (Ross & Ross 1995, 1996; Loydell 1998; Lüning *et al.* 2000; Nielsen 2003*a*). However, precise biostratigraphic dating of high-latitude black shales is hindered by the relative scarcity of graptolites in these settings (Skevington 1974; Zalasiewicz 2001) and the prevalence of non-diagnostic taxa with long ranges (Lüning *et al.* 2000). Nevertheless, where high-latitude, post-glacial black shales contain a sufficient fauna to permit dating, the onset of anoxia can be assigned to the *persculptus* graptolite Zone: e.g. the black shales of the Cedarberg Fm, South Africa, and the Don Braulio Fm, Argentina (Sutcliffe *et al.* 2000, 2001); Batra Fm, Jordan (Armstrong *et al.* 2005); and Murzuq Basin, Libya (Lüning *et al.* 2000). Though Lüning *et al.* (2006) noted that the base of the Batra Fm is diachronous, with its lower member yielding an *acuminatus* graptolite Zone fauna towards the (present-day) North (Armstrong *et al.* 2005, 2006), this is neither inconsistent with the onset of anoxia occurring in the *persculptus* graptolite Zone, nor is it inconsistent with deposition of the Batra Fm as a maximum flooding surface black shale. As the transgression continued into the early Silurian, the oxygen minimum zone would have shoaled further up the shelf (Armstrong *et al.* 2006). The formation of early Silurian black shales, such as at the base of the Qusaiba Shale, Saudi Arabia (Aoudeh & Al-Hajri 1995), is

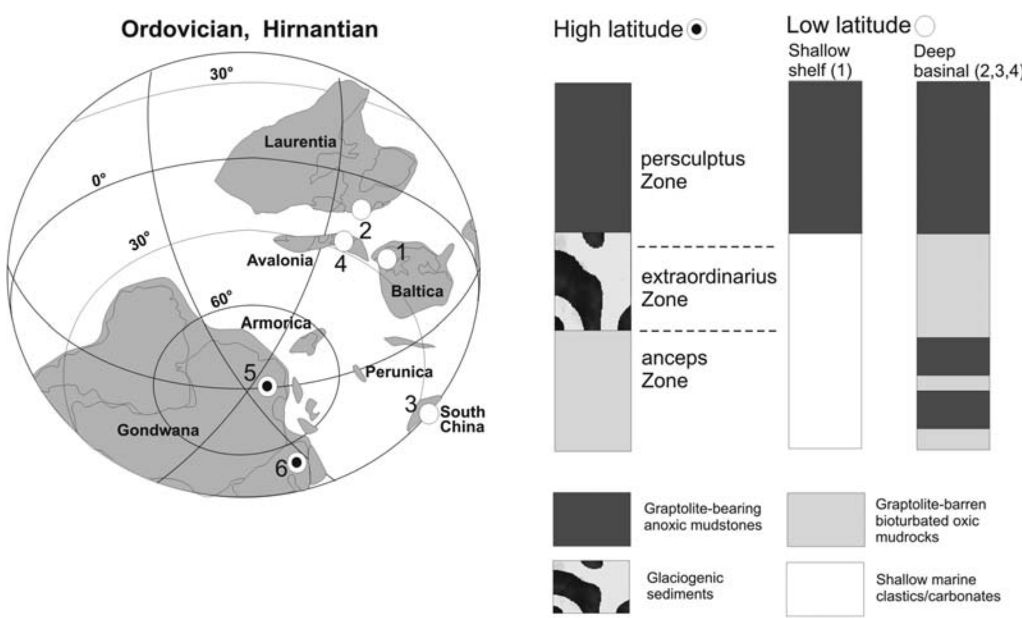

Fig. 4. Schematic lithographic logs showing the onset of transgressive anoxia in different settings during the *persculptus* graptolite Zone anoxic event. Palaeogeographical reconstruction showing the position of continents and associated terranes in the Hirnantian, annotated with localities where black shale is deposited on a maximum flooding surface: 1. Bavnegård Well, Bornholm, Denmark (Bjerreskov 1975); 2. Dob's Linn, Scotland UK (Toghill 1968; Armstrong & Coe 1997; Verniers & Vandenbroucke 2006); 3. Fenxiang, Yingang, Yangtze region, southern China (Mu 1988; Chen *et al.* 2000, 2005); 4. Cwmere Fm, central Welsh Basin, UK (Woodcock *et al.* 1996; Davies *et al.* 1997); 5. Murzuq Basin, Libya (Lüning *et al.* 2000); 6. Batra Fm, Jordan (Armstrong *et al.* 2005). Palaeogeographic reconstructions mainly after Torsvik *et al.* (1998). The relative position of Gondwana, Armorica, Baltica, Avalonia, Laurentia and Siberia are largely unmodified.

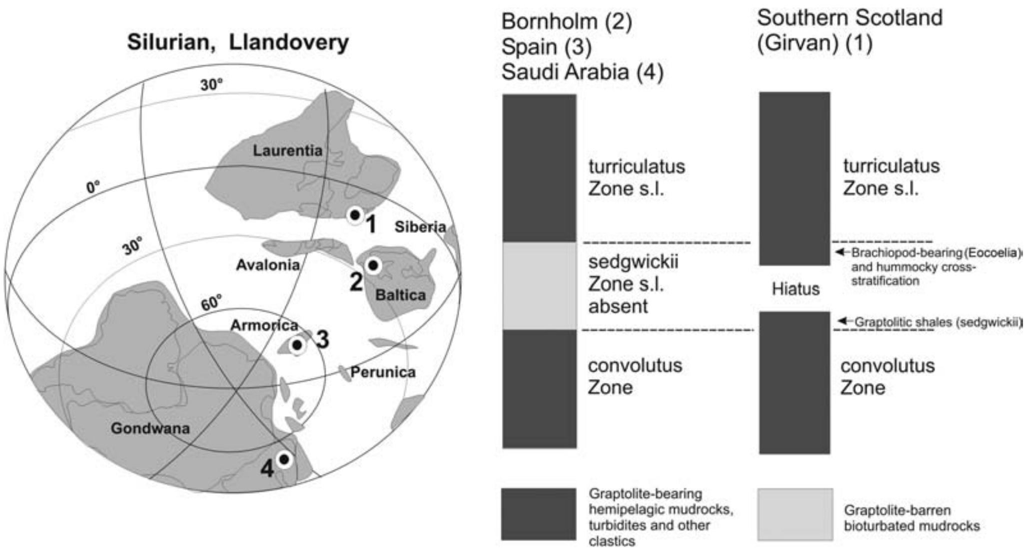

Fig. 5. Schematic lithographic logs showing evidence of regressive oxygenation during the *sedgwickii* graptolite Zone glaciation. Palaeogeographical reconstruction showing the position of continents and associated terranes in the mid-Llandovery, showing global event of deep-water oxygenation: 1. Girvan Group, Scotland, UK (Floyd & Williams 2003); 2. Øleå, Bornholm, Denmark (Bjerreskov 1975); 3. Western Iberian Cordillera, NE Spain (Gutiérrez-Marco & Štorch 1998); 4. Qusaiba Shale, Qalibah Fm, Saudi Arabia (Miller & Melvin 2005; AAP/JAZ/MW unpublished observations). Palaeogeographic reconstructions again mainly after Torsvik *et al.* (1998), with amendments as noted in Figure 4. Also, by the beginning of the Silurian, the amalgamation of some Kazakh crustal terranes probably led to the formation of a substantial landmass north of Tarim and South China (Koren *et al.* 2003). The position of Annamia close to South China and the Karakum–Tajik plate is mainly based on the strong affinities of the late Silurian (Ludlow–Pridoli) brachiopod faunas (Rong *et al.* 1995; Thong-Dzuy *et al.* 2001).

evidence that oceanic anoxia and deposition of maximum flooding surface black shales continued as the transgression continued.

The influx of deglacial meltwater in the oceans of the *persculptus* graptolite Zone may have been critical to the onset of transgressive anoxia: it may have increased marine stratification through the formation of low-salinity surface waters and, by providing a source of nutrients via continental weathering, stimulated marine productivity. This may be analogous to the formation of sapropels in the Neogene Mediterranean Basin (Rohling & Gieskes 1989; Rohling 1994; Scrivner *et al.* 2004). Buoyant, low-salinity surface waters, strengthening the pycnocline in the deglacial Hirnantian Ocean, may have precluded deep-water thermohaline circulation to sufficiently maintain a well-oxygenated sea-floor. Periglacial outwash may have carried sufficient nutrients to fuel the deposition of the 'hot shales' of North Africa and Arabia (cf. Meybeck 1982), which are characterized by a total organic-carbon content of up to 17% (Lüning *et al.* 2000), well above that found in normal black shales.

Some authors have declared that 'hot shale' deposition may be a result of upwelling (Lüning *et al.* 2000, 2005, 2006), but this disaccords with both their widespread, synchronous deposition and with GCMs of Hirnantian circulation (Hermann *et al.* 2003, 2004*a*, *b*). Upwelling is a regionally localized phenomenon and the oxygen minimum zone associated with upwelling zones is only stable on decadal timescales (Wignall 1994). Moreover, meridional and monsoonal coastal upwelling is restricted to low to mid-latitudes (Parrish 1982), so are unlikely to apply to the 'hot shales', which occur at high palaeolatitudes. Meanwhile, end-Ordovician continental configuration is inconsistent with widespread zonal coastal upwelling (Armstrong *et al.* 2006). Zonal upwelling occurs when north or south continental margins lie adjacent to the major zonal wind systems (Parrish 1982). Comparing modern palaeogeographical reconstructions (Scotese & McKerrow 1991; Cocks & Torsvik 2002) with the high-latitude zonal wind predicted in the late Ordovician atmospheric simulations of Parrish (1982) shows that major winds were primarily orthogonal to the

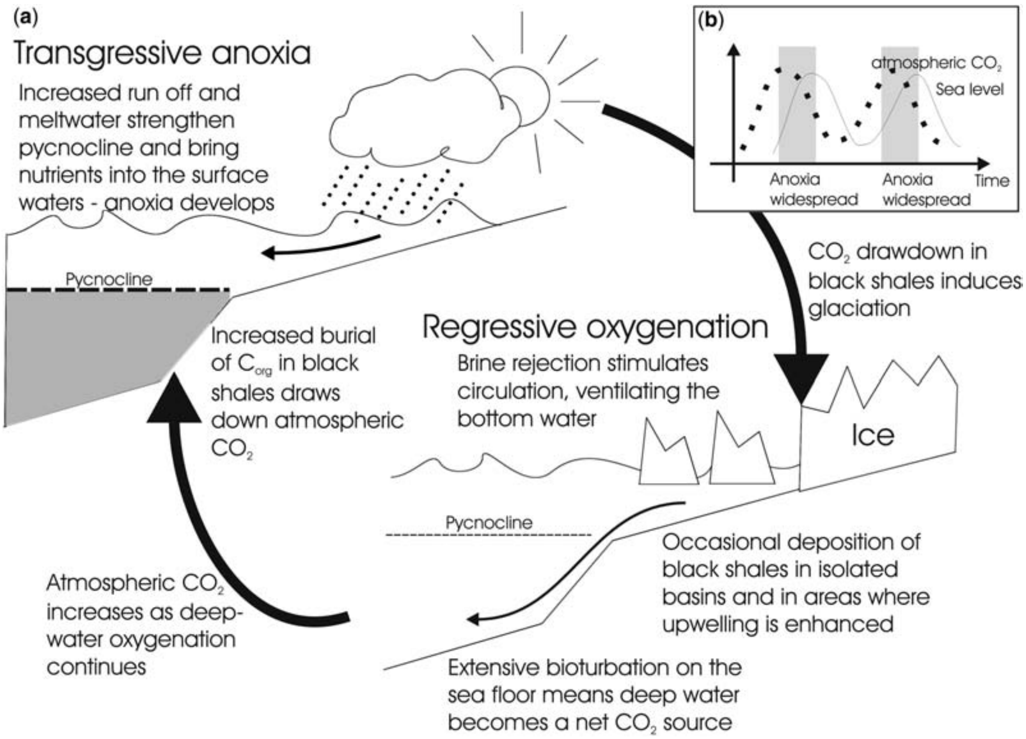

Fig. 6. (**a**) Summary cartoon showing end-member transgressive and regressive oceans in the EPI, outlining a model in which transgressive black shale deposition may serve as a negative-feedback mechanism modulating glacioeustasy (**b**) Graphs showing the postulated relationship between CO_2 temperature and sea-level, given that intervals of transgressive black shale deposition may draw-down significant atmospheric CO_2.

Gondwanan margin, making widespread zonal upwelling untenable. This is borne out by recent, more sophisticated GCMs for the late Ordovician, that show predominantly onshore ocean currents around the North African and Arabian margins of Gondwana (Hermann *et al.* 2003, 2004*a*, *b*). As such, upwelling alone can neither account for the simultaneous onset of globally widespread anoxia in the *persculptus* graptolite Zone nor for the widespread high-latitude occurrence of the most organic-rich shales.

Furthermore, deglacial melting would most likely be to the detriment of the increased thermohaline circulation needed to sustain upwelling. In the Quaternary of the North Atlantic, intervals of meltwater outwash are associated with increased ocean stratification and more sluggish deep-water circulation (Rahmstorf 2002). Instead, an alternative nutrient source may lie in increased continental weathering during deglaciation, providing a major source of both major and trace nutrients (Broecker 1982; Meybeck 1982) and stimulating productivity (as modelled by Kump & Arthur 1999). Given that the locus of glacial melting is focused on the Gondwana palaeocontinent, this nutrient source could explain the relatively increased organic content of high-palaeolatitude black shales compared to those in low palaeolatitude black shales. This would leave anoxia at low palaeolatitudes as a consequence of increased ocean stratification and decreased thermohaline circulation due to high-palaeolatitude ice melting. This, coupled with sediment starvation (cf. Wignall 1991), would lead to an expanded oxygen-minimum zone. Hence, periglacial run-off provides a mechanism for anoxia that would have simultaneously increased global seawater stratification as well as stimulating productivity and export production (see schematic in Fig. 6). This highlights the fundamentally deglacial nature of transgressive black shales in the EPI.

Regressive oxygenation: the *sedgwickii* graptolite Zone event

The *sedgwickii* graptolite Zone is marked by global regression of plausibly glacial origin during which sediments were deposited in well-oxygenated deep water overlying earlier black shales (Table 1; Figs 2 & 5). Graptolites are rarely preserved in extensively bioturbated facies, though graptolites could clearly exist in well-oxygenated waters (Armstrong & Coe 1997; Floyd & Williams 2003; AAP/JAZ/MW unpublished observations). Therefore, bioturbated graptolite-free intervals in otherwise continually graptolitic successions may be taken as evidence of increased sedimentary ventilation, seen in both high- and low-latitude successions in the Iapetus, Rheic and Palaeotethys Oceans (Fig. 5 & references therein). It is clear that the boundary between the preceding *convolutus* graptolite Zone and the *sedgwickii* graptolite Zone is characterized by the development of oxic strata, and that widespread anoxia is again developed by the onset of the *guerichi* graptolite Zone (Loydell 1998).

However, the *sedgwickii* graptolite Zone also contains a distinctive interval of black shale, which is only seen in certain successions from the Iapetus and Rheic Oceans. In UK successions in Wales and Dob's Linn, this thin black shale is sandwiched between a sequence of grey shales and mottled mudstones (e.g. Toghill 1968; Cave 1979). The *sedgwickii* Zone of the Kullatorp core (Västergötland, Sweden) comprises greyish-green mudstones in a succession of otherwise graptolitic black shales. However, the Silvberg and Gulleråsen-Sanden sections of Dalarna contain a finely laminated shale yielding *St. sedgwickii* (Loydell 1998). In Bornholm, Denmark, however, there is an abrupt transition between the highly graptolitic black shale of the *cometa* Band that characterizes the top of the *convolutus* graptolite Zone and a heavily bioturbated, non-graptolitic silty, grey mudstone (Bjerreskov 1975; AAP unpublished observations on Øleå section and collections in the Geological Museum, University of Copenhagen). The *sedgwickii* shale band in the Welsh Basin is generally thought to represent a transgressive black shale (Cave 1979; Baker 1981; Davies & Waters 1995; Woodcock *et al.* 1996). However, it is unlike the transgressive black shales of the *persculptus* graptolite Zone and early Wenlock (Woodcock *et al.* 1996; Lüning *et al.* 2005; Armstrong *et al.* 2005, 2006) in which organic-carbon burial is more profoundly expressed at high palaeolatitudes. Instead, this brief black shale event in the *sedgwickii* Zone is only observed at certain low-latitude settings. There is no major graptolitic shale burial associated with the *sedgwickii* Zone age strata in the Qusaiba Shale, Saudi Arabia (Zalasiewicz *et al.* 2007). This may reflect increased isolation of semi-enclosed basins at low sea-level, suggesting local rather than global significance (e.g. Loydell 1994).

There is good evidence of a regression within the lithofacies deposited during the *sedgwickii* graptolite Zone, and no graptolites have been recovered from the low-latitude successions of the Western Iberian Cordillera, Spain (Gutiérrez-Marco & Štorch 1998), the Prague Basin, Czech Republic (Štorch 1986, 1994), and the Canadian Arctic (Melchin 1989). In Girvan, southern Scotland, UK, the late *sedgwickii* Zone contains shallow-water brachiopods and deposits with hummocky cross-stratification in the Lower Camregan Grits Fm overlying the black shales of the Pencleuch Shale Fm (Floyd & Williams 2003), and in Spengill, Howgill Fells, UK, the *sedgwickii* graptolite Zone contains the only occurrence of limestones and grits in its Llandovery succession (Rickards 1970). The evidence for a regression in UK deep-water strata may correlate with the regressions recognized in the *sedgwickii* s.l. graptolite Zone in sequence stratigraphic analyses of shallow-water facies in Baltoscandia, North America and Siberia (Johnson 1996; Ross & Ross 1996; Yolkin *et al.* 1997), and coincides with the formation of diamictite in Gondwana (Caputo 1998); whilst the overlying *guerichi* graptolite Zone itself appears to mark the onset of extensive marine anoxia (Loydell 1998), which may be linked to a transgression (Fig. 2).

Increased oxygenation of the marine realm in the *sedgwickii* graptolite Zone may be a consequence of high-latitude ice formation stimulating more rapid thermohaline circulation, as is seen in the modern-day Atlantic (Rahmstorf 2002). The *sedgwickii* Zone regression is coincident with diamictite deposition in South America (Caputo 1998; Table 1; Fig. 2), suggesting glacioeustatic control. The formation of marine ice would have resulted in brine rejection, creating cold, dense waters at high latitudes. On sinking, these may have driven a more vigorous deep-water circulation, providing a greater flux of oxygen to the deep oceans (see Fig. 6), consistent with the well-ventilated deep-water facies seen in glacial maxima during the EPI (Fig. 2; Brenchley 1988). The global cessation of anoxic facies at the end of the *convolutus* graptolite Zone and their return in the *guerichi* graptolite Zone reflects a third-order change in depositional style, consistent with a glacioeustatic control on oceanic redox state (Church & Coe 2003).

A simple model for carbon burial and glacioeustasy in the EPI

During the EPI, there was a fundamental link between glacioeustatic sea-level change and the burial of organic carbon in deglacially transgressive black shales, which may have represented a negative feedback mechanism that served to stabilize climate (Fig. 6), and prevented the onset of runaway greenhouse conditions. Given that sea-level may represent a proxy for atmospheric temperature, which itself is a function of pCO_2, the deposition of globally extensive black shales on maximum flooding surfaces may have served to slow the initial warming after the glacial maxima by drawing down CO_2 from the ocean–atmosphere system. This would sustain the EPI and prevent onset of greenhouse conditions that characterized most of the Early Palaeozoic (Frakes *et al.* 1992; Gibbs *et al.* 2000; Montañez 2002; Church & Coe 2003).

This model for deposition of black shales due to periglacial meltwater increasing both productivity and ocean stratification predicates that oceanic anoxia was intimately linked to glacioeustasy. Black shale deposition in transgressions may have been significant to influence cooling, and therefore a regression, by drawing down atmospheric carbon (see the schematic graph in Fig. 6). Likewise, the onset of well-oxygenated oceans due to brine rejection driving deep-water circulation may have served to prevent organic carbon burial to sustain fully glacial conditions, which might have led to another transgression. With global marine oxygenation linked to ice formation and melting, we infer a strong link between organic carbon burial in black shales, sea level and atmospheric CO_2 during the EPI. This model now needs to be rigorously tested against both the sedimentary record of the EPI and by developing theoretical models of the carbon budget.

Black shale deposition and the EPI carbon cycle

Though we have clearly shown a strong link between black shale deposition and deglacial transgressions, relating anoxia and carbon-burial flux is not straightforward. Models of the carbon cycle show a significant increase in carbon burial as black shales close to the Ordovician–Silurian boundary (Fig. 1c). Meanwhile, Ronov *et al.* (1980) estimated that the amount of organic carbon buried in Ordovician and Silurian black shales is comparable to that in Permo-Carboniferous strata, a time when the organic reservoir may have exerted a significant influence on atmospheric CO_2 (e.g. Bruckschen *et al.* 1999). As the EPI corresponds to a major low in shelf-carbonate deposition, organic carbon burial in black shales may have been critical to regulating the carbon cycle (Fig. 1; Patzkowsky *et al.* 1997). The increase in atmospheric O_2 during this interval is consistent with increased organic-carbon burial (Fig. 1a, c; cf. Berner 2003; Catling & Clare 2005), empirically linking black shale deposition and atmospheric change. Though we have shown that black shale burial occurs in transgressions, the lateral extent of black shale is unclear, making it hard to estimate the carbon burial flux from rock volume.

The oxygenation–depth profile of EPI oceans is largely unknown. Oxic–anoxic transitions occur in open-ocean settings, demonstrating that this is not a phenomenon exclusive to restricted basins or epicontinental seas (cf. Porębska & Sawłowicz 1997). Similarly, anoxia may be developed in shelf settings relatively close to the storm wave-base, such as in the Qusaiba Shale of Saudi Arabia, where anoxic or dysoxic facies alternate with bioturbated mudstones and facies yielding benthic faunas (Miller & Melvin 2005). Precisely how shallow anoxic conditions may extend in the EPI is unclear (cf. Pancost *et al.* 1998). Whether these transgressive anoxic events represent shoaling of an expanded oxygen minimum zone onto the shelf, or whether there was widespread whole oceanic anoxia in the EPI, remains uncertain.

We concur with Cramer & Saltzman (2005, 2007) that the deposition of organic carbon in epicontinental black shales cannot account for positive $\delta^{13}C$ excursions in the Silurian. As they noted, widespread deposition of shales in epicontinental seas does not coincide with these excursions. Neither do our data show evidence for increased carbon burial in deep-water settings with strong oceanic influence during any of the positive $\delta^{13}C$ excursions (Table 1; Fig. 2). We also contest the suggestion of upwelling and increased carbon burial as an explanation for positive $\delta^{13}C$ excursions in the EPI (e.g. Young *et al.* 2005). All positive $\delta^{13}C$ excursions in the EPI are best explained by increased weathering of shallow marine carbonates in regressions (e.g. Kump *et al.* 1999; Melchin & Holmden 2006) as noted in the Appendix. Young *et al.* (2005) argued that the Guttenberg regression was synchronous with biomarker evidence for photic-zone anoxia based on the data of Pancost *et al.* (1998). This however represents a miscorrelation. The high-resolution stratigraphy of Ludvigson *et al.* (2004) demonstrates that the interval of photic zone anoxia identified by Pancost *et al.* (1998) corresponds to the Spects Ferry Member of the Platteville Fm. The Spects Ferry Member underlies the Guttenberg Limestone, preceding the EPI, whilst the Guttenberg regression corresponds to lithological evidence of a more-oxic interval (cf. Ludvigson *et al.* 2004). As noted above, there is no direct evidence for increased organic carbon preservation or productivity during the positive $\delta^{13}C$ excursions of the EPI (cf. Chen *et al.* 2005). Because of this, and the inability of upwelling to explain the synchronous onset of global anoxia, we attribute anoxia to increased deglacial outwash causing oceanic stratification (Fig. 6).

It is still unclear how black shale burial varies with regard to the burial of other facies associated with atmospheric CO_2 drawdown. On timescales greater than 1000 years, carbonate burial provides a sink for CO_2 (Elderfield 2002). Continental silicate weathering draws down CO_2 over geological timescales and may have been the key driver of changes in atmospheric CO_2 over geologically long timescales (Holland 1978; Berner 1991; Raymo 1991; Kump *et al.* 1999; Cohen *et al.* 2004). As continental weathering is thought to increase with greater temperatures (Berner *et al.* 1983; Velbel 1993; Hovius 1998), and the rate of erosion appears to be greater in unstable (transitional) climates than in stable greenhouse or icehouse climates (e.g. Shuster *et al.* 2005), one would expect a greater CO_2 drawdown due to weathering in transgressions. Our model for drawdown of CO_2 in transgressive anoxia due to increased freshwater runoff from the continents would augment this, complementing drawdown of CO_2 to the oceans by silicate weathering and limestone burial (e.g. Kump *et al.* 1999). Improved constraints on the relation between weathering, carbonate deposition, black shale burial and changes in global temperature would further improve our understanding of EPI climate.

Comparison of black shale and carbonate burial in the EPI

Black shale burial can be compared to carbonate deposition and changes in global temperature by relating the oxic/anoxic stratigraphy of Figure 2 to Primo/Secundo (P/S) and Humid/Arid (H/A) cycles. These cycles relate changes in carbonate deposition to changes in temperature and deep-water circulation. P/S and H/A cycles were recognized in the Silurian by Jeppsson (1990, 1997) and Bickert *et al.* (1997) respectively. These cycles have recently been reviewed and synthesized by Cramer & Saltzman (2005; 2007), who viewed Silurian climate as alternating between two end-member oceanographic regimes. The first regime is characterized by cooler (P), wetter (H) climates with high sea-levels; argillaceous limestone deposition took place in shallower successions and black shales were deposited on the continental shelf, with oxic deep waters. The other regime is characterized by warmer (S), more arid (A) climates with lower sea-level; reefs formed in shallow successions and limestones were deposited on the shelf with black shales deposited in anoxic open oceans. It should, however, be noted that Jeppsson (1990, 1997) and Bickert *et al.* (1997) differ in their views on where and when anoxia occur. Bickert *et al.* (1997) suggested the open oceans were anoxic throughout both H and A episodes with anoxia shoaling onto the shelf in H episodes. Jeppsson (1990, 1997) proposed oxic deep waters occurred in P episodes with anoxia occurring on the shelf due to high productivity in these episodes; conversely, he proposed that S episodes were characterized by well-oxygenated shelf conditions and anoxia in the open oceans.

There is no simple relationship between the oxic–anoxic stratigraphy of the British Isles and either P/S or H/A cycles. In the Ordovician, Kaljo *et al.* (1999; 2004) recognized humid and arid episodes in both the mid–late Caradoc, which was predominantly anoxic, and the Ashgill, which was predominantly oxic (Fig. 3). Likewise, observations of glacial maxima and anoxia do not accord well with the P/S model. For example, the Spirodden Secundo episode lasts from the *persculptus* graptolite Zone until the *argenteus* graptolite Zone (Aldridge *et al.* 1993), a time recognized as being a warmer deglacial interval. This episode has a similar duration to the anoxic conditions in the UK (*persculptus–magnus* graptolite zones interval) as shown in Figure 2. In contrast, the Malmøykalven Secundo episode (Aldridge *et al.* 1993) corresponds to the *sedgwickii* graptolite Zone, a period of globally extensive oxic conditions and glaciation, as discussed above. Moreover, the P/S episodes recognized in the Llandovery (Aldridge *et al.* 1993) do not correspond well with glacioeustatic sea-level changes or episodes of organic carbon burial in black shales (Fig. 2; Loydell 1998). There was a relatively low rate of limestone burial during the EPI (Fig. 1b), and glacial maxima show a clearer link between changes in oceanic redox state than they do with either P/S or H/A cycles. So, we suggest that ocean anoxia seems to reflect changes in atmospheric CO_2 and temperature more clearly than does carbonate deposition.

Discussion

The model works well for the clearly deglacial anoxic events in the EPI, especially those in the *clingani*, *persculptus* and *centrifugus* graptolite zones (Fig. 2). Likewise, there is clear evidence for increased deep-water ventilation and the deposition of well-oxygenated mudstones in glaciations themselves (Figs 2 & 5). However, it only addresses how black shale deposition may serve as a negative feedback to stabilize EPI climate rather than providing a mechanism for the onset and termination of ice formation in the EPI. Recognizing repeated glacial maxima within the EPI, rather than just focusing on the Hirnantian event, significantly furthers our understanding of Early

Palaeozoic climate. Characterizing the lithostratigraphic patterns associated with each glacial maximum has established a consistent set of events associated with ice-sheet formation and retreat. The factors associated with ice formation within individual EPI glacial maxima can be potentially inferred from these 'event stratigraphies'. The differences in scale between each of the glacial maxima may be used to infer which factors were most important for ice formation in the EPI. That is, the most important factors controlling ice formation are likely to be most strongly expressed in large events such as the Hirnantian glacial maximum, but only weakly expressed in smaller events. Once the factors which control ice formation in glacial maxima have been established, it may be possible to infer what was responsible for the onset and termination of the EPI.

We have employed stratigraphic correlation of sub-graptolite zone resolution to recognize individual glacial maxima within the EPI and their associated lithostratigraphic changes. By combining isotopic data with glacioeustatic curves and lithostratigraphic patterns, there is considerable potential for developing a highly resolved Ordovician–Silurian global event stratigraphy. By comparison, biostratigraphy alone offers comparatively poor resolution and global coverage. The first appearances of many graptolites are diachronous (cf. Williams *et al.* 2003, 2004; Cooper & Sadler 2004). Likewise, the relative scarcity of graptolites in cool waters and in shallow environments (Skevington 1974; Finney & Berry 1997; Loydell 1998; Zalasiewicz 2001) may preclude accurate correlation between high and low latitudes (e.g. Lüning *et al.* 2000), and also between graptolite and conodont or shelly-fossil biostratigraphies (e.g. Mullins & Aldridge 2004). Contrastingly, carbon isotope stratigraphies appear to show good correlations between differing facies and palaeogeographical settings, allowing global correlation (e.g. Underwood *et al.* 1997; Melchin & Holmden 2006; Kaljo *et al.* 2007). Moreover, the strong coupling of both positive carbon isotope excursions with changes in deep-water redox conditions and glacioeustasy (Figs 2 & 6) represents a method of correlating third-order sequence stratigraphic changes, potentially providing a new tool for Early Palaeozoic stratigraphy. Likewise, this model for formation of transgressive black shales and their role in carbon burial (Fig. 6) may extend to other intervals. For example, the Toarcian oceanic anoxic event in the Jurassic saw continental run-off corresponding to the onset of anoxia, which induced CO_2 drawdown and subsequent cooling (Cohen *et al.* 2004).

In the EPI, neither the occurrence of glacial maxima nor oxic–anoxic transitions are regularly spaced (Fig. 2) and these events may therefore have been externally forced. The lack of observed cyclicity in the occurrence of glacial maxima suggests that the negative feedback due to CO_2 drawdown in transgressive black shale deposition was insufficient to create regular, self-sustaining glacial–interglacial cycles. The long intervals of anoxic marine conditions (e.g. late Caradoc, early Silurian and late Telychian–early Wenlock) and predominantly oxic marine conditions (e.g. early Caradoc, Ashgill, Telychian) may suggest that there was a second-order, possibly tectonic control on ocean redox conditions (see also Leggett 1980; Leggett *et al.* 1981). Likewise, the distribution of the currently recognized glacial maxima may be of second-order rather than third-order periodicity. Such second-order forcing, possibly by the opening and closing of oceanic gateways (e.g. Smith & Pickering 2003; Armstrong this volume), or drawdown of CO_2 due to increased silicate weathering in orogenies (Kump *et al.* 1999), may ultimately be responsible for the conditions that facilitated ice formation in the EPI.

Conclusions

Recognizing the EPI as a long-lived interval revises our understanding of Early Palaeozoic climate, showing a long-lived icehouse in an interval previously thought to be dominated by greenhouse conditions (cf. Brenchley *et al.* 1994; Gibbs *et al.* 2000; Montañez 2002; Church & Coe 2003; Royer 2006). Its *c.* 30-million-year duration makes it comparable to other long-lived icehouses such as those in the Cenozoic, Permo-Carboniferous and even the Neoproterozoic. All of these events are characterized by waxing and waning of ice-sheets on different timescales with potentially different forcing and feedback mechanisms dependent on timescale. Moreover, each of these icehouses represents a markedly different solution to the Earth's carbon budget, and the locus and importance of organic burial varied considerably between them (cf. Fig. 1). Though atmospheric CO_2 levels appear to have controlled global temperature over geological time (Royer 2006), each of these icehouses is characterized by a markedly different carbon cycle, which needs to be understood in its own terms.

Though there are many uncertainties shrouding our understanding of glaciation in this interval, the EPI is notably different from those of the modern oceans: it may have represented a time when the deposition of black shales in conditions of marine anoxia played a significant role in mediating the carbon cycle and climate.

We wish to thank David Harper and an anonymous reviewer for their helpful and insightful comments. AAP wishes to thank Eddie Blackett, Andrea Snelling (both Leicester & BGS), Nigel Woodcock & Barrie Rickards (Cambridge) and Jakob Vinther (Copenhagen) for showing him around *persculptus* and *sedgwickii* graptolite Zone sections in Wales, Sedbergh and Bornholm, and for providing access to their collections from these areas. Likewise, we thank Merrell Miller (Saudi Aramco) for providing access to boreholes of late Aeronian–early Telychian strata from Saudi Arabia. Cambridge Earth Science contribution 8775.

Appendix: Choice/interpretation of datasets and correlations

Details of individual datasets used in this study and our interpretations of them are discussed in turn below.

Stratigraphic framework: our correlations follow those of Cooper & Sadler (2004) for the Ordovician, and Melchin *et al.* (2004) for the Silurian, although we correlate the Llandovery–Wenlock boundary to Ireviken datum 2 (see next paragraph). In addition, we refer to Nõlvak *et al.* (2006) for correlation of the Ordovician timescale in Estonia to the global standard. We refer to other stratigraphic compilations in the text as necessary and assume that all major isotopic excursions are globally synchronous.

The International Commission on Stratigraphy website notes that the correlation of the Llandovery–Wenlock boundary GSSP is 'imprecise' (www.stratigraphy.org). To resolve this, the stratigraphy of the late Telychian–early Wenlock interval has received much attention of late (e.g. Jeppsson 1997; Loydell *et al.* 2003; Munnecke *et al.* 2003; Mullins & Aldridge 2004; Cramer & Saltzman 2005, 2007). The absence of taxonomically identifiable graptolites in the GSSP (Mullins & Aldridge 2004) makes correlation to graptolite zones uncertain (Melchin *et al.* 2004). However, the GSSP has a good conodont and microfossil stratigraphy, although the position of the golden spike does not correspond to the base of any particular biozone (Mabillard & Aldridge 1985; Mullins & Aldridge 2004). Instead, recent works have correlated this boundary at a slightly younger level, namely Ireviken datum 2 (e.g. Loydell *et al.* 2003; Calner *et al.* 2004). This represents the boundary between the lower and upper *Ps. bicornis* conodont zonal levels (Jeppsson 1997), which is close to the base of the *murchisoni* graptolite Zone (Loydell *et al.* 2003). This level has been suggested as a correlatable level for the boundary on the International Commission on Stratigraphy website (www.stratigraphy.org).

Most original works on Ordovician deposits (Table 2) correlate these strata to the British stages (cf. Fortey *et al.* 1995, 2000). As such, we refer to these stages throughout this paper (the relations between the British stages and the international stages of Cooper & Sadler [2004] are shown in Fig. 2). However, we use the term Hirnantian *sensu* Cooper & Sadler (2004) as this stage is well-defined with good global correlation. We note that the definition and correlation of the British Ordovician stages is not unproblematic (Fortey *et al.* 1995, 2000; Cooper & Sadler 2004). The recent placement of the GSSPs for these stages reflects improved Ordovician biostratigraphy. The recently named Sandbian and Katian Stages of the Ordovician are defined on the well-correlated first appearances of the graptolites *Nemagraptus gracilis* and *Ensigraptus caudatus*, even though the first appearance of these graptolites is locally diachronous (cf. Williams *et al.* 2003, 2004). Therefore, we feel that the historical correlation of glacial deposits to the British stages, and our use of the UK oxic–anoxic stratigraphy, justify our reference to these 'old-fashioned' terms and we wish to highlight that use of old terms does not necessarily reflect the employment of outmoded correlations.

Criteria for recognizing glacial maxima: The glacial maxima identified in the EPI (Table 1) are recognized using an argument similar to that employed by Brenchley *et al.* (1994). Namely, glacial maxima occur when rapid regressions are accompanied by synchronous oxygen and carbon evidence of cooling, if there are contemporaneous glacial deposits. Glaciations may be recognized from either the deposition of diamictites containing glaciogenic clasts, ice-rafted debris in distal marine settings, or from glacial erosive features (Eyles 1993). However, evidence of ice may not necessarily be evidence of glacial maxima, as ice-sheets may persist through interglacials. Also, an extensive unconformity of Caradoc–Hirnantian age persists through much of Africa and Arabia (Destombes *et al.* 1985; Sutcliffe 2001), potentially removing evidence of glaciations in this interval. Likewise, correlation between high-latitude glacial deposits and equivalent low-latitude strata may be hindered by (a) the low-abundance of graptolites in high-latitude environments (Lüning *et al.* 2000; Zalasiewicz 2001), and (b) the general absence of limestone-hosted shelly faunas in these settings (e.g. Walker *et al.* 2002). However, if the co-occurrence of ice formation with regressions and positive $\delta^{13}C$ and $\delta^{18}O$ excursions is not contradicted by biostratigraphic data, then it seems more parsimonious to consider them to be related to a glaciation rather than being caused by separate events.

Sea-level curves: The sea-level curves illustrated in Figure 2 are based on sequence stratigraphic analyses of shallow-water facies. These may be 'calibrated' to the depths of such facies in modern environments (Ross & Ross 1996), though such estimates may also vary according to sediment flux or local topography (Orr 2001). Nevertheless, other methods for estimating sea-level change possess inherent uncertainties. Faunally derived sea-level curves may represent changes in palaeoenvironment rather than deepening *per se* (Orr 2001). For example, 'quantitative' sea-level curves based on conodont assemblages do not produce consistent results in different environments (e.g. Zhang *et al.* 2006). Glacial maxima within the EPI may be associated with

Table 2. *Evidence for ice formation during the EPI; palaeolatitudes inferred from palaeogeographical reconstructions for the Caradoc, Hirnantian and Llandovery–Wenlock boundary, quoted to within ±5° N/S; stratigraphic nomenclature reflects the original author's usage*

Stage	Age	Location	Palaeolat.	Evidence of ice	Evidence for age
CARADOC *sensu* Fortey *et al.* (1995, 2000)	'Llandeilo-Caradoc boundary' Hamoumi (1999)	Lower Ktaoua Formation, Zagora, Morocco	80° S	glacial pavement with polished surface displaying *roche moutonnée*-like forms, undulating surfaces, graze, score & nail-shaped groove joints (Beuf *et al.* 1971; Hamoumi 1999)	surface forms base of L. Ktaoua Fm, which has ?*gracilis–clingani* graptolite Zone age (Destombes *et al.* 1985) based on comparison of trilobite & brachiopod fauna with UK and Bohemia; overlies 1st Bani Formation of 'Llandeilo' age (Destombes *et al.* 1985) with erosive contact
	'Lower Caradoc' Hamoumi (1999)	Lower Ktaoua Formation, Zagora, central Anti-Atlas, Morocco	80° S	surface remnants at corrie heads displaying battered & scoured surfaces, nivation hollows and thermokarst, on top of glaciotectonised and jointed glaciomarine sediments (Beuf *et al.* 1971; Hamoumi 1999)	within L. Ktaoua Fm, which has ?*gracilis–clingani* graptolite Zone age (Destombes *et al.* 1985), based on comparison of trilobite & brachiopod fauna with UK and Bohemia
	Caradoc (Pickerill *et al.* 1979)	Gander Bay Tillites, Davidsville Group, Newfoundland, Canada	65° S†	diamictites and locally abundant dropstones (Pickerill *et al.* 1979)	oldest strata in the Davidsville Group contain conodonts of Llanvirn–Llandeilo age; diamictites immediately underlie graptolitic slate of Caradoc age (Pickerill *et al.* 1979)
	Caradoc (Schenck & Lane 1981)	White Rock Fm, Nova Scotia, Canada	65° S†	marine-rafted tillite with clasts in small lenses and dropstone fabrics in varvites (Schenck & Lane 1981), quartz meta-arenites showing polished striations and groves on facets (Schenck 1972)	tillite overlain by 'poorly preserved, limited [graptolite] fauna of Caradoc or younger age' (Schenck 1972; Schenck & Lane 1981)
CARADOC or ASHGILL	'middle Caradoc–Ashgill boundary' Hamoumi (1999)	Touririne Fm, Eastern Anti-Atlas, Morocco	75° S	'frost dominated cold tidal [surface]... display (*sic*) ice wedges, desiccation polygons and karstification' Hamoumi (1999)	Lower Touririne Sandstone member contains trilobite fauna comparable to '*peltifer* graptolite Zone' fauna of Letná Fm, Bohemia; Upper Touririne sandstone member coeval with strata of *clingani*–? *complanatus* graptolite zone age; Touririne Fm unconformably overlain by Hirnantian tillites; stratigraphy in Destombes *et al.* (1985)

(*Continued*)

Table 2. *Continued*

Stage	Age	Location	Palaeolat.	Evidence of ice	Evidence for age
ASHGILL (excluding Hirnantian *sensu* Cooper & Sadler 2004)	'Upper Ordovician' Legrand (1985)	Tamadjert Fm*, Western Hoggar, Algeria	60° S	buried landscapes show glacial landforms, with striations, drumlins, vestiges of moraines, traces of solifluction, ?pingos; terrestrial and marine tillite deposits (Beuf *et al.* 1971; Biju-Duval *et al.* 1981; Legrand 1985)	unconformably overlies strata of Caradoc age (Biju-Duval *et al.* 1981); marine facies may contain late Caradoc trilobites, brachiopods and graptolites (Gatinskiy *et al.* 1966); upper part of formation contains middle–late Llandovery graptolites (Legrand 1970)
	'Upper Ordovician' Tucker & Reid (1973)	Sierra Leone	50° S	ice-drop tillites with carbonate boulders (Tucker & Reid 1973)	lithological similarity to and correlation with similar deposits in Guinea which are overlain by Llandovery graptolite shales (Tucker & Reid 1973)
	Ashgill (Doré 1981)	Tillite de Feuguerolles, Normandy, France	40° S	ice-drop tillites and diamictites with glacially striated clasts (Doré & Le Gall 1973; Doré 1981)	conformably underlain by strata containing Caradoc age trilobites and other fossils (Robardet *et al.* 1972; Doré & Le Gall 1973; Doré 1981); conformably overlain by strata yielding latest Ordovician–earliest Silurian graptolite fauna (Phillipot & Robardet 1971; Doré 1981)
	'Late Ordovician' Deynoux & Trompette (1981)	Taoudeni Basin, West Africa	70° S	terrestrial and marine tillites in the area near the Hodh with striated boulders; glacially reworked deposits with outwash fans 'similar to the Icelandic sandur' (Deynoux & Trompette 1981); 'micro-cordons' that probably represent subglacial eskers in englacial tunnels; structures similar to *fentes minces* (Deynoux & Trompette 1981); glacial pavements and *roches moutonées* with striations, furrows and crescentic fractures in the Hodr; glaciotectonic features including ice-push ridges and *fractures en gradin* (Biju-Dival *et al.* 1974)	glacial deposits have erosive disconformity at their base (Deynoux & Trompette 1981; Deynoux, Sougy & Trompette 1985) overlying the upper part of Supergroup 2, which has an age near the Cambro-Ordovician boundary based on inarticulate brachiopods and trace fossils (Legrand 1969); base comparable with Caradoc–Ashgill unconformity in the Hoggar, Tassilis & Anti-Atlas (Deynoux & Trompette 1981); glacial deposits conformably but ?diachronously overlain by graptolite faunas of Upper Ashgill–middle Llandovery age (Underwood *et al.* 1998)

HIRNANTIAN *sensu* Cooper & Sadler (2004)	*extraordinarius* graptolite Zone acme (Sutcliffe *et al.* 2000, 2001)	Northern Africa: Upper 2nd Bani Fm, Anti-Atlas Mts, Morocco; Djebel Serraf Fm, Ougarta Mts, Algeria	75° S	synchronous, large-scale tillite and diamictite deposition; two phases of regionally extensive glaciomarine shelf sequences and subglacial erosive surfaces; ice-contact fans, ice-rafted debris (Sutcliffe *et al.* 2000, 2001; see also Hamoumi 1999)	*Hirnantia* fauna within glaciogenic deposits, and in underlying formations (erosive contacts); disconformably overlain by strata containing Rhuddanian graptolites (Destombes *et al.* 1985; Sutcliffe *et al.* 2000, 2001)
	extraordinarius graptolite Zone acme (Sutcliffe *et al.* 2000, 2001)	Melez Chograne & Memouniat Fms, Libya	75° S	glaciomarine shelf deposits, ice-rafted debris and erosive surfaces covered by ice-contact deposits (Havlíček & Massa 1973; Sutcliffe *et al.* 2001)	*Hirnantia* fauna throughout succession, overlain by Llandovery graptolites (Havlíček & Massa 1973; Sutcliffe *et al.* 2001)
	extraordinarius graptolite Zone acme (Sutcliffe *et al.* 2000, 2001)	Tichit glacial group, the Hodh, Mauritania	70° S	glacially striated dropstones, diamictites (Deynoux & Trompette 1981; Ghienne 2003)	dropstones coexist with graptolites of Upper Ashgill age (Underwood *et al.* 1998)
	extraordinarius graptolite Zone acme (Sutcliffe *et al.* 2000, 2001)	Pakhuis Fm, South Africa	15° S	tillites & diamictites, two subglacial erosive surfaces with striated pavements and boulders, ice-rafted debris (Rust 1981; Sutcliffe *et al.* 2000, 2001)	*Hirnantia* fauna in conformably overlying Cedarberg Fm (Sutcliffe *et al.* 2001)
	?Hirnantian	Tabuk Fm, Arabian peninsula	50° S	diamictites & tillites with some striated, faceted and polished clasts; boulder pavements with striations (McClure 1978)	tillite interfingers with late Caradoc age graptolite shale also containing trilobites of late Caradoc or early Ashgill age (Young 1981); overlying Qusaiba Shale contains a Rhuddanian age graptolite fauna (Lüning *et al.* 2000)
	Hirnantian (Armstrong *et al.* 2005)	Ammar Fm, southern Jordan	50° S	tillite; glacial unconformity at base and two episodes of glacial incision; conglomerates with glacially faceted and striated clasts (Abed *et al.* 1993)	conformably overlain by *persculptus* graptolite Zone fauna (Armstrong *et al.* 2005)
	Hirnantian (Caputo 1998)	Don Braulio Fm, Argentina	15° S‡	diamictite some striated, faceted and polished pebbles and cobbles (Büggish & Astini 1993)	overlain by *Hirnantia* fauna (Sutcliffe *et al.* 2001)

(*Continued*)

Table 2. *Continued*

Stage	Age	Location	Palaeolat.	Evidence of ice	Evidence for age
	?Hirnantian (Caputo 1998)	Iapó Fm, Paraná Basin, Brazil	25° S	diamictites with faceted and striated clasts (Maack 1957; Rocha-Campos 1981)	lithological comparison with South African and Argentinian tillites (Caputo 1998); Iapó Fm discordantly overlies rhyolites of the Castro Group dated at 450 ± 25 Ma (Bigarella 1970); correlation with interfingering Vila Maria Fm suggests diamictite overlain by early Llandovery palynomorph and shelly fauna (Caputo & Crowell 1985)
	Hirnantian	Prague Basin, Czech Republic	55° S	two intervals of diamictite deposition (Brenchley & Štorch 1989)	conformably underlain by *Mucronaspis* fauna and *anceps* Zone graptolites; conformably overlain by Hirnantian fauna (Štorch & Mergl 1989)
LLANDOVERY (Rhuddanian)	?Rhuddanian	San Gabán–Cancañiri–Zapla Fms, Bolivia, Argentina & Peru	55° S	widely extensive diamictites with striated and faceted clasts (Crowell *et al.* 1981; Caputo & Crowell 1985; Díaz-Martínez & Grahn 2007)	oldest diamictite horizon overlain by Aeronian chitinozoan fauna and underlain by Rhuddanian chitinozoan ; (Díaz-Martínez & Grahn 2007); these formations unconformably overlie Caradoc strata showing evidence of Ashgillian deformation (Crowell *et al.* 1981)
	'Upper Ordovician or Lower Silurian' (Kennedy 1981)	Stoneville & Beaver Cove Fms, Newfoundland, Canada	60° S†	diamictite beds; dropstones probably derived by iceberg rafting (Kennedy 1981)	Stoneville & Beaver Cove Fms are coeval (Kennedy 1981); former underlain by poorly preserved corals of Upper Ordovician or Lower Silurian age (McCann & Kennedy 1974) and lithological correlatives of its upper part have yielded Llandovery age fossils (Eastler 1969; Kennedy 1981)
LLANDOVERY (Aeronian)	*gregarius* graptolite Zone (Caputo 1998)	Nhamundá Fm, Amazonas Basin Brazil	60° S	diamictite; ice-push & ice-shear deformation structures (Carozzi *et al.* 1973; Caputo 1998)	diamictite immediately overlain by *gregarius* Zone graptolite fauna and chitinozoan fauna (Grahn & Paris 1992; Caputo 1998)

	'late Aeronian–early Telychian' (Caputo 1998)	Nhamundá Fm, Amazonas Basin, Brazil	60° S	diamictite; ice-push & ice-shear deformation structures (Carozzi *et al.* 1973; Caputo 1998)	overlies *gregarius* Zone fauna; shales lateral to tillites yield an early Telychian chitinozoan fauna (Caputo 1998)
	?Aeronian	San Gabán–Cancañiri–Zapla Fms, Bolivia, Argentina & Peru	60° S	widely extensive diamictites with striated and faceted clasts (Crowell *et al.* 1981; Caputo & Crowell 1985; Díaz-Martínez & Grahn 2007)	overlies shales yielding Aeronian chitinozoans (Díaz-Martínez & Grahn 2007), overlain by shales and a younger diamictite horizon
	Llandovery (Caputo 1998)	Ipu Fm, Parnaíaba Basin & Cariri Valley, Brazil	70° S	three diamictite layers (Caputo & Crowell 1985; Grahn & Caputo 1992); faceted pebbles (Kegel 1953)	interfingers with Tianguá Fm, which contains Early Silurian chitinozoans and acritarchs (Caputo & Lima 1984); individual diamictites may correlate with the better-dated diamictites in the Nhamundá Fm (Grahn & Caputo 1992)
LLANDOVERY (Telychian, including *centrifugus* Zone)	late Telychian (Grahn in Cramer & Saltzman 2007)	Nhamundá Fm, Amazonas Basin, Brazil	70° S	diamictites and tillites; ice-push & ice-shear deformation structures (Carozzi *et al.* 1973; Caputo 1998)	Late Telychian–early Wenlock chitinozoan fauna in interfingering shales (Caputo 1998); first appearance of chitinozoa *M. magaritana* above the youngest tillite (Grahn in Cramer & Saltzman 2007)
	Late Telychian; (Díaz-Martínez 2007)	San Gabán–Cancañiri–Zapla Fms, Bolivia, Argentina & Peru	65° S	widely extensive diamictites with striated and faceted clasts (Crowell *et al.* 1981; Caputo & Crowell 1985; Díaz-Martínez & Grahn 2007)	youngest diamictite conformably overlain by Sacla limestone, which has early Wenlock age based on occurrence of the conodont *O. sagitta rhenana* (Díaz-Martinez 2007); however, acritarchs and chitinozoans in intercalated shale horizons suggest a Llandovery–Wenlock boundary age (Suárez-Soruco 1995); this diagnosis may suggest an older age than Ireviken Datum 2 (see Appendix)

*Synonym of Felar Felar Fm.
†This part of Nova Scotia is thought to have been on the margin of West Africa at this time (Kennedy 1981).
‡Position of the Argentine Precordillera poorly constrained at this interval.

faunal turnover and changes in oceanic temperature and oxygenation. As such, faunally derived sea-level curves do not necessarily provide independent evidence of glacioeustasy in this interval. We only make passing reference to Loydell (1998), even though this offers well-defined evidence of Silurian sea-level change with good stratigraphic control. However, there is no curve defined using a comparable method for the Ordovician. And, as Loydell's (1998) sea-level curve uses deposition of graptolite shale as a criterion for establishing sea-level change, employing it would preclude an independent test of the relationship between sea-level and black shale distribution during the EPI.

Though we have used sea-level curves for the Ordovician and Silurian by different authors (Ross & Ross 1996; Nielsen 2003*a*), both are compiled using the same method and correlate sequences in North America and Baltoscandia. As the Iapetus Ocean closed, there may have been an increased local-tectonic component in the Laurentian record of sea-level change during the EPI (e.g. McKerrow *et al.* 2000). Nevertheless, correlation between two palaeocontinents reduces the chance of conflating relative tectonic changes with global changes in sea-level, and significant global events should register above local noise. The Nielsen (2003*a*) sea-level curve for the Ordovician shows a strong correlation with the equivalent sea-level curve by Ross & Ross (1995), but offers better stratigraphic resolution. Meanwhile, the Ross & Ross (1996) curve for the Silurian employs a method consistent with that used by Nielsen (2003*a*) in the Ordovician. The original Ross & Ross (1996) sea-level curve has poor biostratigraphic control in the late Telychian (Loydell 1998), with the authors referring to an undifferentiated *crenulata* Zone between the *griestoniensis* and *centrifugus* zones. This interval can be differentiated into four graptolite zones (e.g. Loydell *et al.* 1998). As such, Figure 2 illustrates an amended version of the Ross & Ross (1996) curve based on the recorrelation of their original stratigraphy by Loydell (1998).

The sequence stratigraphic patterns observed by Ross & Ross (1996) may be consistent with 20–60 m changes in sea-level in less than 1–2 Ma. The rates and frequency of sea-level change during the EPI (Ross & Ross 1996; Nielsen 2003*a*, *b*) are consistent with third-order sequence stratigraphic cycles. They are therefore more likely glacially than tectonically forced (Church & Coe 2003).

Oxygen isotopes: The oxygen isotope data presented in Table 1 are obtained from the shells of brachiopods. These were selected on the basis that they showed no trace element or microstructural evidence of significant diagenetic alteration (Brenchley *et al.* 1994; Marshall *et al.* 1997; Azmy *et al.* 1998; Tobin *et al.* 2005). Modern brachiopods secrete a low-Mg calcite shell at or near isotopic equilibrium with seawater (Lowenstam 1961; Carpenter & Lohmann 1995; James *et al.* 1997), which tends to resist diagenesis (Marshall *et al.* 1997; Azmy *et al.* 1998). The isotopic composition of their shells shows little deviation due to vital effects at the present day (Carpenter & Lohmann 1995). Analysis of multi-taxa assemblages in the Silurian suggests that vital effects may not have been significant in the Palaeozoic (Samtleben *et al.* 2001). Hence, these fossil data have been regarded as representative of the isotopic composition of Early Palaeozoic seawater (e.g. Veizer *et al.* 1997; Samtleben *et al.* 2001).

Positive $\delta^{18}O$ excursions can be achieved by decreases in temperature or increases in salinity (e.g. Hays & Grossman 1991). The latter can be achieved due to increased ice volume or decreased freshwater input, and both may occur along with decreased temperature in glaciations (e.g. Azmy *et al.* 1998; Tobin *et al.* 2005). Though changes in salinity alone have been argued to account for the positive isotope excursions observed in this interval (e.g. Samtleben *et al.* 1996; Bickert *et al.* 1997), such changes represent salinity change of *c.* 14‰, which is an implausibly large change that cannot be tolerated by brachiopods (Azmy *et al.* 1998). As such, we interpret these positive excursions as representing decreases in temperature, which may be accompanied by smaller increases in salinity. Therefore, positive $\delta^{18}O$ excursions can be related to glaciations if consistent with other evidence (e.g. Brenchley *et al.* 1994; Azmy *et al.* 1998).

Carbon isotopes: The isotopic curves illustrated in Figure 2 represent a consistent record of the $\delta^{13}C$ of carbonates throughout the EPI. These curves were compiled using bulk rock carbonates in the Baltic region. These strata have a well-resolved stratigraphy correlated to graptolite, conodont and chitinozoan zones (e.g. Loydell *et al.* 1998, 2003; Loydell & Nestor 2005; Nõlvak *et al.* 2006). In this interval, the Estonian chronostratigraphic nomenclature is well-established across Baltoscandia and widely used for correlation of carbonate-hosted assemblages (Cooper & Sadler 2004; Melchin *et al.* 2004). This allows precise correlation between sea-level curves and isotope data.

The $\delta^{13}C$ curves we illustrate were compiled by a single research group using consistent sampling strategies and analytic techniques on bulk rock carbonates (for methods, see Kaljo *et al.* 1997, 1998, 2001). These data show little evidence for diagenetic alteration (Kaljo *et al.* 1997, 1998, 2001). The curves in Figure 2 are consistent with each other. Individual excursions show good accord with both organic and inorganic carbon-isotope records derived in different regions (e.g. Underwood *et al.* 1997; Kump *et al.* 1999; Melchin & Holmden 2006). The major positive excursions highlighted in Table 1 and Figure 2 are recognized in the more-or-less continuous record of carbon isotopes from the shells of Silurian brachiopods (e.g. Azmy *et al.* 1998). They also occur in the bulk rock data from the Ordovician of Laurentia (e.g. Patzkowsky *et al.* 1997; Saltzman & Young 2005) and the compilation for the Palaeozoic of the Great Basin, USA (Saltzman 2005). The similarity of the $\delta^{13}C$ curves in Figure 2 to these other $\delta^{13}C$ curves highlights that the bulk-rock curves of Baltica record global perturbations in the carbon cycle.

Kump & Arthur (1999) and Kump *et al.* (1999) show that positive carbon-isotope excursions can be achieved by (a) increasing productivity, (b) increasing the burial flux of organic carbon, or (c) by positive excursions in the $\delta^{13}C$ value of riverine input into the marine carbon reservoir due to increased terrestrial carbonate weathering. These alternatives can be distinguished by analysis of coupled patterns of organic and inorganic carbon isotopes (cf. Kump & Arthur 1999; Kump *et al.* 1999). For example, coupled organic and inorganic $\delta^{13}C$ data are available for the Hirnantian glaciation, and these positive $\delta^{13}C$ excursions have been interpreted as representing changes in weathering (Kump *et al.* 1999; Melchin & Holmden 2006). This excursion occurs during a major regression (e.g. Brenchley *et al.* 2004; Melchin & Holmden 2006), which exposed shallow marine carbonates to terrestrial weathering, resulting in a more positive $\delta^{13}C$ value of river waters (Kump *et al.* 1999). Given that all the positive $\delta^{13}C$ excursions of the EPI correspond to lowstands in cooler intervals with decreased organic carbon burial in deep-water settings (Table 1; Fig. 2), all positive $\delta^{13}C$ excursions may reasonably be interpreted as being due to increased weathering of shallow carbonates exposed in regressions.

The positive $\delta^{13}C$ excursion isotope excursion associated with the Hirnantian glaciation is hard to reconcile with increased productivity or organic preservation (cf. Brenchley *et al.* 1994). This event is coincident with a mass extinction (e.g. Sutcliffe *et al.* 2000; Chen *et al.* 2005), when there is no evidence of increased organic burial in even the deepest-water facies (e.g. Armstrong & Coe 1997). We therefore believe it is best to consider the positive carbon-isotope excursions of the EPI to represent cooler events if they are coincident with regression (e.g. Patzkowsky *et al.* 1997; Azmy *et al.* 1998; Kaljo *et al.* 2003; Tobin *et al.* 2005; Johnson 2006), and that these excursions may be related to glaciations if consistent with other evidence.

Oxic–anoxic stratigraphy: Anoxic intervals are recognized from the occurrence of laminated hemipelagic mudrocks in deep-water settings (i.e. below storm wave base), which often contain graptolites. Graptolites are organic walled macrozooplankton and the majority of their fossil record comes from distal, anoxic mudrocks (Chapman 1991; Underwood 1992; Finney & Berry 1997). They may also be sporadically found in oxic facies, should they have undergone rapid burial. For example, *Stimulograptus sedgwickii* occurs in well-ventilated sandstones and siltstones in the Girvan area, UK (Floyd & Williams 2003), and in the shelf successions of the Llandovery area, Wales, UK (Cocks *et al.* 1984). Likewise, tiny graptolite fragments have been reported from rocks showing evidence of bioturbation (e.g. Armstrong & Coe 1997; Mullins & Aldridge 2004). Thus, the presence of graptolites in well-laminated, dark-grey or black mudrocks is evidence of anoxia rather than graptolite palaeoecology (cf. Berry *et al.* 1987). Similarly, the absence of macrofossil graptolites in poorly laminated and/or burrowed paler grey shales is more typical of oxygenated bottom waters and sediments.

The oxic–anoxic stratigraphy for the EPI presented here (Fig. 3 and refs therein) is derived from correlating anoxic intervals in the deep-water record of UK successions. These successions are located in the Welsh Basin and Southern Uplands of Scotland, which occur on the Iapetus margins of Avalonia and Laurentia respectively (Zalasiewicz 2001). They have a well-established, high-resolution stratigraphy that allows such oxic–anoxic transitions to be recognized at a sub-graptolite zone resolution (e.g. Verniers & Vandenbroucke 2006). Thus, if anoxic facies are deposited simultaneously in the Welsh Basin and Southern Uplands, they represent at least an Iapetus-wide anoxic event (Fig. 2). Where intervals of anoxia in the Southern Uplands and Welsh Basin do not correlate, it may be that sediment redox conditions represent local rather than oceanic events. Leggett (1980) made a similar compilation for the Early Palaeozoic of the UK, employing stage level correlations. However, our higher resolution oxic–anoxic stratigraphy allows individual events to be correlated at a biozone level (e.g. Fig. 3).

The basis of the UK record as a reliable record of global marine anoxia requires consideration of the changing depositional settings of both the Welsh Basin and Southern Uplands. We select data from intervals where these strata were deposited in shelf and/or deep-basin environments. To establish the global extent, we also correlate this stratigraphy with redox changes recognized in the deep-water record of the Rheic and/or Palaeothethys Oceans. As far as we are aware, the record of marine anoxia in the deep-water facies of the UK represents the only well-dated, continuous succession where the oxic–anoxic stratigraphy has been sufficiently documented to assemble a composite oxic–anoxic stratigraphy for the EPI.

The Welsh Basin was a restricted basin on the eastern margin of Avalonia. Its depositional setting and sedimentary history are reviewed by Woodcock (2000) and Zalasiewicz (2001). Local changes in freshwater run-off, nutrient input or upwelling may have induced localized anoxic events by altering productivity and stratification. Its sedimentary record stretches from the Cambrian to latest Silurian. Nevertheless, the widespread volcanism prior to the mid-Caradoc significantly disrupted patterns of marine topography, subsidence and deposition (Woodcock 1990). This resulted in a more ambiguous and locally variable pattern of basin redox conditions at this time (cf. Leggett 1980). Once sediment input outpaced subsidence in the late Silurian (King 1994; Woodcock 2000), the basin became increasingly shallow and it rapidly filled with sediment. The oxic–anoxic stratigraphy of the Welsh Basin correlates extremely well with similar stratigraphies where available for the deep-water successions of the Howgill Fells and Lake District, Northern England (cf. Rickards 1970; Hutt 1974; Rickards & Woodcock 2005). Thus, the Welsh Basin provides a well-resolved record of the oxic–anoxic stratigraphy of eastern Avalonia throughout the EPI.

In contrast, the Moffat Shale Group of the Southern Uplands is commonly thought to represent an ocean floor environment approaching a trench (Leggett *et al.* 1979; Leggett 1987). It may have been susceptible to changes in upwelling, which could have induced localized anoxia by increasing export production (e.g. Finney & Berry 1997). The Southern Uplands record of the EPI is contained within an accretionary prism formed from Iapetus thrust-slices during the Caledonian Orogeny (Leggett *et al.* 1979; Leggett 1987; Strachan 2000). The succession has an early Caradoc to late Llandovery age (Leggett 1980, 1987; Strachan 2000). Subsequently, the Moffat Shale Group was overlain by the massive flysch deposits of the Gala and Hawick groups of late Llandovery to Wenlock age (White *et al.* 1991). At a larger scale, the mudstones of the Moffat Shale Group comprise a generally distal, condensed succession of Ordovician and early Llandovery age, with slightly more expanded and proximal facies in the mid- and late Llandovery. So, rather than being a restricted basin, the Southern Uplands provide a well-resolved record of open marine conditions throughout all but the terminal part of the EPI.

The major anoxic events of the Welsh Basin correlate well with those from the Southern Uplands where data are available (Fig. 3). Hence, there is no reason to believe that the late Llandovery–Wenlock of the Welsh Basin is unrepresentative of the Iapetus Ocean redox conditions, especially as synchronous changes are seen in northern England (cf. Rickards 1970; Rickards & Woodcock 2005). Thus, the oxic–anoxic stratigraphies of the UK basins (Fig. 3), from which we compiled the summary oxic–anoxic stratigraphy (Fig. 2), probably represent the best record available of oxic–anoxic transitions in low-latitude deep waters during the EPI.

References

Abed, A. M., Makhlouf, I. M., Amireh, B. S. & Khalil, B. 1993. Upper Ordovician glacial deposits in southern Jordan. *Episodes*, **16**, 316–328.

Ainsaar, L., Meidla, T. & Martma, T. 1999. Evidence for a widespread carbon isotopic event associated with late Middle Ordovician sedimentological and faunal changes in Estonia. *Geological Magazine*, **136**, 49–62.

Aldridge, R. J., Jeppsson, L. & Dorning, K. J. 1993. Early Silurian oceanic episodes and events. *Journal of the Geological Society, London*, **150**, 501–513.

Aoudeh, S. M. & Al-Hajri, S. A. 1995. Regional distribution and chronostratigraphy of the Qusaiba Member of the Qalibah Formation in the Nafud Basin, northwestern Saudi Arabia. *In*: Al-Husseini, M. I. (ed.) *Geo '94, The Middle East Petroleum Geosciences*, vol. 1. Gulf PetroLink, Manama, Bahrain, 143–154.

Armstrong, H. A. & Coe, A. L. 1997. Deep sea sediments record the geophysiology of the end Ordovician glaciation. *Journal of the Geological Society, London*, **154**, 929–934.

Armstrong, H. A., Turner, B. R., Makhlouf, I. M., Weedon, G. P., Williams, M., Al Smadi, A. & Abu Salah, A. 2005. Origin, sequence stratigraphy and depositional environment of an Upper Ordovician (Hirnantian) deglacial black shale, Jordan. *Palaeogeography, Palaeoclimatology, Palaeoecology*, **220**, 273–289.

Armstrong, H. A., Turner, B. R., Makhlouf, I. M., Weedon, G. P., Williams, M., Al Smadi, A. & Abu Salah, A. 2006. Reply to 'Origin, sequence stratigraphy and depositional environment of an upper Ordovician (Hirnantian) deglacial black shale, Jordan'. *Palaeogeography, Palaeoclimatology, Palaeoecology*, **230**, 356–360.

Arrhenius, S. 1896. On the influence of carbonic acid in the air upon the temperature on the ground. *Philosophical Magazine and Journal of Science*, **41**, 237–275.

Azmy, K., Veizer, J., Bassett, M. G. & Copper, P. 1998. Oxygen and carbon isotopic composition of Silurian brachiopods: Implications for coeval seawater and glaciations. *Geological Society of America Bulletin*, **110**, 1499–1512.

Baker, S. J. 1981. The graptolite biostratigraphy of a Llandovery outlier near Llanystumdwy, Gwynedd, North Wales. *Geological Magazine*, **118**, 355–365.

Barker, S., Higgins, J. A. & Elderfield, H. 2003. The future of the carbon cycle: review, calcification response, ballast and feedback on atmospheric CO_2. *Philosophical Transactions of the Royal Society of London, series A*, **361**, 1977–1999.

Barnes, C. R. & Bolton, T. E. 1998. The Ordovician–Silurian boundary on Manitoulin Island, Ontario, Canada. *Bulletin of the British Museum, Natural History, Geology*, **43**, 247–253.

Berner, R. A. 1991. A model for atmospheric CO_2 over Phanerozoic time. *American Journal of Science*, **291**, 339–376.

Berner, R. A. 1994. GEOCARB II: A revised model of atmospheric CO_2 over Phanerozoic time. *American Journal of Science*, **294**, 56–91.

Berner, R. A. 1998. The carbon cycle and CO_2 over Phanerozoic time: the role of land plants. *Philosophical Transactions of the Royal Society, series B*, **353**, 75–82.

Berner, R. A. 2001. Modelling atmospheric O_2 over Phanerozoic time. *Geochimica et Cosmochimica Acta*, **65**, 685–694.

Berner, R. A. 2003. The long-term carbon cycle, fossil fuels and atmospheric composition. *Nature*, **426**, 323–326.

Berner, R. A. 2006. GEOCARBSULF: A combined model for Phanerozoic atmospheric O_2 and CO_2 over Phanerozoic time. *Geochimica et Cosmochimica Acta*, **70**, 5653–5664.

Berner, R. A. & Canfield, D. E. 1989. A new model for atmospheric oxygen over Phanerozoic time. *American Journal of Science*, **289**, 333–361.

Berner, R. A. & Kothavala, Z. 2001. Geocarb III: A revised model of atmospheric CO_2 over Phanerozoic time. *American Journal of Science*, **301**, 182–204.

Berner, R. A. & Raiswell, R. 1983. Burial of organic carbon and pyrite sulfur in sediments over Phanerozoic time: a new theory. *Geochimica et Cosmochimica Acta*, **47**, 855–862.

BERNER, R. A., LASAGA, A. C. & GARRELS, R. M. 1983. The carbonate–silicate geochemical cycle and its effect on atmospheric carbon dioxide over the past 100 million years. *American Journal of Science*, **283**, 641–683.

BERRY, W. B. N., WILDE, P. & QUINBY-HUNT, M. S. 1987. The oceanic non-sulfidic oxygen minimum zone; a habitat for graptolites? *Bulletin of the Geological Society of Denmark (Meddelelser fra Dansk Geologisk Forening)*, **35**, 103–114.

BEUF, S., BIJU-DUVAL, B., DE CHARPAL, O., ROGNON, P., GARIEL, O. & BENNACEF, A. 1971. *Les grès du Paléozoïque inférieur au Sahara (Sédimentation et discontinuities, evolution structurale d'un craton).* Publication de l'Institut Français Pétrole, **18**.

BICKERT, T., PÄTZOLD, J., SAMTLEBEN, C. & MUNNECKE, A. 1997. Paleoenvironmental changes in the Silurian indicated by stable isotopes in brachiopod shells from Gotland, Sweden. *Geochimica et Cosmochimica Acta*, **61**, 2717–2730.

BIGARELLA, J. J. 1970. Continental drift and palaeocurrent analysis. Second Gondwana Symposium, Proceedings and Papers. Council for Scientific and Industrial Research, South Africa, 73–97.

BIJU-DUVAL, B., DEYNOUX, M. & ROGNON, P. 1974. Essai d'interprétation de 'fractures en gradins' observées dans les formations glaciaires Précambriennes et Ordoviciennes du Sahara. *Revue de Geographie Physique et de Geologie Dynamique*, **26**, 503–512.

BIJU-DIVAL, B., DEYNOUX, M. & ROGNON, P. 1981. Late Ordovician tillites of the Central Sahara. *In*: HAMBREY, M. J. & HARLAND, W. B. (eds) *Earth's Pre-Pleistocene Glacial Record.* Cambridge University Press, Cambridge, 99–107.

BJERRESKOV, M. 1975. Llandoverian and Wenlockian graptolites from Bornholm. *Fossils and Strata*, **8**, 1–94.

BRENCHLEY, P. J. 1988. Environmental changes close to the Ordovician–Silurian boundary. *Bulletin of the British Museum of Natural History* (*Geology*), **43**, 377–385.

BRENCHLEY, P. J. & ŠTORCH, P. 1989. Environmental changes in the Hirnantian (upper Ordovician) of the Prague Basin, Czechoslovakia. *Geological Journal*, **24**, 165–181.

BRENCHLEY, P. J., MARSHALL, J. D. & CARDEN, G. A. F. *ET AL*. 1994. Bathymetric and isotopic evidence for a short-lived Late Ordovician glaciation in a greenhouse period. *Geology*, **22**, 295–298.

BRENCHLEY, P. J., CARDEN, G. A., HINTS, L. *ET AL*. 2003. High-resolution isotope stratigraphy of Late Ordovician sequences: constraints on the timing of bio-events and environmental changes associated with mass extinction and glaciation. *Geological Society of America, Bulletin*, **115**, 89–104.

BROECKER, W. S. 1982. Glacial to interglacial changes in ocean chemistry. *Progress in Oceanography*, **11**, 151–197.

BRUCKSCHEN, P., OESMANN, S. & VEIZER, J. 1999. Isotope stratigraphy of the European Carboniferous: proxy signals for ocean chemistry, climate and tectonics. *Chemical Geology*, **161**, 127–163.

BRUNTON, F. R., SMITH, L., DIXON, O. A., COPPER, P., NESTOR, H. & KERSHAW, S. 1998. Silurian reef episodes, changing seascapes, and paleobiogeography. *In*: LANDING, E. & JOHNSON, M. E. (eds) *Silurian Cycles, Linkages of Dynamic Stratigraphy with Atmospheric, Oceanic, and Tectonic Changes.* New York State Museum Bulletin, **491**, 265–282.

BÜGGISH, W. & ASTINI, R. 1993. The Late Ordovician ice age: new evidence from the Argentine Precordillera. *In*: FINDLAY, R. H., UNRUG, R., BANKS, M. R. & VEEVERS, J. J. (eds) *Gondwana Eight – Assembly, Evolution and Dispersal*. Balkema, Rotterdam, 439–447.

BUTTERFIELD, N. J. 1997. Plankton ecology and the Proterozoic–Phanerozoic transition. *Paleobiology*, **23**, 247–262.

CALNER, M. & ERIKSSON, M. E. 2006. Silurian research at the crossroads. *GFF*, **128**, 73–74.

CALNER, M., JEPPSSON, L. & MUNNECKE, A. 2004. The Silurian of Gotland – Part I: Review of the stratigraphic framework, event stratigraphy, and stable carbon and oxygen isotope development. *Erlanger Geologische Abhandlungen, Sonderband*, **5**, 113–131.

CAPUTO, M. V. 1998. Ordovician–Silurian glaciations and global sea-level changes. *In*: LANDING, E. & JOHNSON, M. E. (eds) *Silurian Cycles, Linkages of Dynamic Stratigraphy with Atmospheric, Oceanic, and Tectonic Changes.* New York State Museum Bulletin, **491**, 15–25.

CAPUTO, M. V. & CROWELL, J. C. 1985. Migration of glacial centers across Gondwana during Paleozoic Era. *Geological Society of America, Bulletin*, **96**, 1020–1036.

CAPUTO, M. V. & LIMA, E. C. 1984. Estratigrafia, idade e correlação do Grupo Serra Grande – Bacia do Parnaíba. *Congresso Brasileiro de Geologia*, **33**, 740–753.

CAROZZI, A. V., PAMPLONA, H. R. P., CASTRO, J. C. & CONTREIRAS, C. J. A. 1973. Ambientes deposicionais e evolução tecto-sedimentar da seção elástica paleozóica da Bacia do Médio Amazonas. *Congresso Brasileiro de Geologia*, **27**, 279–314.

CARPENTER, S. J. & LOHMANN, K. C. 1995. $\delta^{18}O$ and $\delta^{13}C$ values of modern brachiopods. *Geochimica et Cosmochimica Acta*, **59**, 3749–3764.

CATLING, D. C. & CLAIRE, M. 2005. How Earth's atmosphere evolved to an oxic state: A status report. *Earth and Planetary Science Letters*, **237**, 1–20.

CAVE, R. 1979. Sedimentary environments of the basinal Llandovery of mid-Wales. *In*: HARRIS, A. L., HOLLAND, C. H. & LEAKE, B. E. (eds) *The Caledonides of the British Isles – Reviewed*. Special Publication of the Geological Society, London, **8**, 517–26.

CAVE, R. & DIXON, R. J. 1993. The Ordovician and Silurian of the Welshpool area. *In*: WOODCOCK, N. H. & BASSETT, M. G. (eds) *Geological Excursions in Powys, Central Wales*. Geological Series – National Museum of Wales, **14**, 51–84

CHAMBERLIN, T. C. 1899. An attempt to frame a working hypothesis of the cause of glacial periods on an atmospheric basis. *Journal of Geology*, **7**, 545–584.

CHAPMAN, A. J. 1991. How are they preserved? *In*: PALMER, D. & RICKARDS, R. B. (eds) *Graptolites:*

Writing in the Rocks. Fossils illustrated, vol. 1. The Boydell Press, Woodbridge, UK, 6–11.

CHEN X., RONG JIAYU, C. E. MITCHELL, D. A. T. HARPER, FAN, JUNXUAN, ZHAN, RENBIN, ZHANG, YUANDONG, LI, RONGYU & WANG, YI 2000. Late Ordovician to earliest Silurian graptolite and brachiopod biozonation from the Yangtze region, South China, with a global correlation. *Geological Magazine*, **137**, 623–650.

CHEN, X., MELCHIN, M. J., SHEETS, H. D., MITCHELL, C. E. & FAN, J.-X. 2005. Patterns and Processes of latest Ordovician graptolite extinction and recovery based on data from South China. *Journal of Paleontology*, **79**, 842–861.

CHURCH, K. D. & COE, A. L. 2003. Processes controlling relative sea-level change and sediment supply. *In*: COE, A. L. (ed.) *The Sedimentary Record of Sea-Level Change*. Cambridge University Press, Cambridge, 99–117.

COCKS, L. R. M. & TORSVIK, T. H. 2002. Earth geography from 500 to 400 million years ago: A faunal and palaeomagnetic review. *Journal of the Geological Society of London*, **159**, 631–644.

COCKS, L. R. M., WOODCOCK, N. H., RICKARDS, R. B., TEMPLE, J. T. & LANE, P. D. 1984. The Llandovery Series of the type area. *Bulletin of the British Museum (Natural History): Geology*, **38**, 131–182.

COHEN, A. S., COE, A. L., HARDING, S. M. & SCHWARK, L. 2004. Osmium isotope evidence for the regulation of atmospheric CO_2 by continental weathering. *Geology*, **32**, 157–160.

COOPER, R. A. & SADLER, P. M. 2004. The Ordovician Period. *In*: GRADSTEIN, F. M., OGG, J. G. & SMITH, A. G. (eds) *A Geologic Time Scale 2004*. Cambridge University Press, Cambridge, 165–187.

COPPER, P. 1994. Ancient reef ecosystem expansion and collapse. *Coral Reefs*, **13**, 3–11.

CRAMER, B. D. & SALTZMAN, M. R. 2005. Sequestration of ^{12}C in the deep ocean during the early Wenlock (Silurian) positive carbon isotope excursion. *Palaeogeography, Palaeoclimatology, Palaeoecology*, **219**, 333–349.

CRAMER, B. D. & SALTZMAN, M. R. 2007. Fluctuations in epeiric sea carbonate production during Silurian positive carbon isotope excursions: A review of proposed paleoceanographic models: *Palaeogeography, Palaeoclimatology, Palaeoecology*, in press.

CROWELL, J. C., SUÁREZ-SORUCO, R. & ROCHA-CAMPOS, A. C. 1981. The Silurian Cancañiri (Zapla) Formation of Bolivia, Argentina and Peru. *In*: HAMBREY, M. J. & HARLAND, W. B. (eds) *Earth's Pre-Pleistocene Glacial Record*. Cambridge University Press, Cambridge, 902–907.

CROWLEY, T. J. & BERNER, R. A. 2001. CO_2 and climate change. *Science*, **292**, 870–872.

DAVIES, J. R. & WATERS, R. A. 1995. The Caban Conglomerate and Ystrad Meurig Grits Formation – nested channels and lobe switching on a mud dominated latest Ashgill to Llandovery lope-apron, Welsh Basin, UK. *In*: PICKERING, K. T., HISCOTT, R. N., KENYON, N. H., RICCI LUCCHI, F. & SMITH, R. D. A. (eds) *Atlas of Deep Water Environments: Architectural Style in Turbidite Systems.* London: Chapman & Hall, 182–93.

DAVIES, J. R., FLETCHER, C. J. N., WATERS, R. A., WILSON, D., WOODHALL, D. G. & ZALASIEWICZ, J. A. 1997. Geology of the country around Llanilar and Rhayader. *Memoir of the British Geological Survey*, Sheets 178 and 179 (England and Wales). HMSO, London.

DAVIES, J. R., WATERS, R. A., WILBY, P. R., WILLIAMS, M. & WILSON, D. 2003. *Geology of Cardigan and Dinas Island district – a brief explanation of the geological map. Sheet explanation of the British Geological Survey.* 1: 50000 sheet 193 (including part of sheet 210) Cardigan & Dinas Island (England & Wales). Keyworth, Nottingham, British Geological Survey.

DESTOMBES, J., HOLLAND, H. & WILLEFERT, S. 1985. Lower Palaeozoic rocks of Morocco. *In*: HOLLAND, C. H. (ed.) *Lower Palaeozoic of north-western and west-central Africa*. Lower Palaeozoic Rocks of the World, **4**, 91–337, John Wiley & Sons, Chichester.

DEYNOUX, M. & TROMPETTE, R. 1981. Late Ordovician tillites of the Taodeni Basin, West Africa. *In:* HAMBREY, M. J. & HARLAND, W. B. (eds) *Earth's pre-Pleistocene Glacial Record*. Cambridge University Press, 89–96.

DEYNOUX, M., SOUGY, J. & TROMPETTE, R. 1985. Lower Palaeozoic rocks of west Africa and the western part of central Africa. *In*: HOLLAND, C. H. (ed.) *Lower Palaeozoic of North-Western and West-Central Africa.* Lower Palaeozoic Rocks of the World, **4**, 337–497, John Wiley & Sons, Chichester.

DIAZ-MARTINEZ, E. 2007. The Sacta Limestone Member (early Wenlock): cool-water, temperate carbonate deposition at the distal foreland of Gondwana's active margin, Bolivia. *Palaeogeography, Palaeoclimatology, Palaeoecology*, in press.

DIAZ-MARTINEZ, E. & GRAHN, Y. 2007. Early Silurian glaciation along the western margin of Gondwana (Peru, Bolivia, and northern Argentina): Palaeogeographic and geodynamic setting. *Palaeogeography, Palaeoclimatology, Palaeoecology*, in press.

DORÉ, F. & LE GALL, J. 1973. Presence et position stratigraphique de la tillite Ordovicienne dans le Maine (E. du Massif Armoricain). *Bulletin de la Société Géologique de France*, **15**, 32–33.

DORÉ, F. 1981. The late Ordovician tillite in Normandy (Armorican Massif) *In*: HAMBREY, M. J. & HARLAND, W. B. (eds) *Earth's Pre-Pleistocene Glacial Record*. Cambridge University Press, Cambridge, 582–584.

EASTLER, T. E. 1969. Silurian geology of the Change Islands and eastern Notre Dame Bay, Newfoundland. *Memoir of the American Association of Petroleum Geologists*, **12**, 425–432.

ELDERFIELD, H. 2002. Climate change: Carbonate mysteries. *Science*, **296**, 1618–1621.

EVANS, D. A. D. 2003. A fundamental Precambrian–Phanerozoic shift in Earth's glacial style? *Tectonophysics*, **375**, 353–385.

EYLES, N. 1993. Earth's glacial record and its tectonic setting. *Earth Science Reviews*, **35**, 1–248.

FINNEY, S. C. & BERRY, W. B. N. 1997. New perspectives on graptolite distributions and their use as indicators of platform margin dynamics. *Geology*, **25**, 919–922.

FLOYD, J. D. & WILLIAMS, M. 2003 (for 2002). A revised correlation of Silurian rocks in the Girvan district, SW

Scotland. *Transactions of the Royal Society of Edinburgh, Earth Sciences*, **25**, 383–392.

FORTEY, R. A. & COCKS, L. R. M. 2003. Palaeontological evidence bearing on global Ordovician–Silurian continental reconstructions. *Earth Science Reviews*, **61**, 245–307.

FORTEY, R. A. & COCKS, L. R. M. 2005. Late Ordovician global warming – The Boda Event. *Geology*, **33**, 405–408.

FORTEY, R. A., HARPER, D. A. T., INGHAM, J. K., OWEN, A. W. & RUSHTON, A. W. A. 1995. A revision of Ordovician series and stages from the historical type area. *Geological Magazine*, **132**, 15–30.

FORTEY, R. A., HARPER, D. A. T., INGHAM, J. K., OWEN, A. W., PARKES, M. A., RUSHTON, A. W. A. & WOODCOCK, N. H. 2000. A revised correlation of Ordovician rocks in the British Isles. *Geological Society of London Special Report*, **24**, 1–83.

FRAKES, L. A., FRANCIS, J. E. & SYKTUS, J. I. 1992. *Climate Modes of the Phanerozoic*. Cambridge University Press, Cambridge.

GATINSKIY, Y. G., KLOCHKO, V. P., ROZMAN, K. S. & TROFIMOV, D. M. 1966. Novyye dannyye po stratigrafii paleozoyskikh otlozheniy yuzhnoy Sakhary. *Akadwmii Nauk SSSR, Doklady*, **170**, 1154–1157.

GENSEL, P. G. & EDWARDS, D. 2001. *Plants Invade the Land: Evolutionary and Environmental Perspectives*. Columbia University Press, New York.

GHIENNE, J.-F. 2003. Late Ordovician sedimentary environments, glacial cycles, and post-glacial transgression in the Taoudeni Basin, West Africa. *Palaeogeography, Palaeoclimatology, Palaeoecology*, **189**, 117–145.

GIBBS, M. T., BICE, K. L., BARRON, E. J. & KUMP, L. R. 2000. Glaciation in the early Paleozoic 'greenhouse'; the roles of paleogeography and atmospheric CO_2. *In*: HUBER, B. T., MACLEOD, K. G. & WING, S. L. (eds) *Warm Climates in Earth History*. Cambridge University Press, Cambridge, 386–422.

GOLDMAN, D., LESLIE, S. A., NÕLVAK, J. & YOUNG, S. 2005. The Black Knob Ridge section, southeastern Oklahoma, USA: a possible Global Stratotype-Section and Point (GSSP) for the base of the Middle Stage of the Upper Ordovician Series. www.stratigraphy.org/BKR.pdf.

GRAHN, Y. & CAPUTO, M. V. 1992. Early Silurian glaciations in Brazil. *Palaeogeography, Palaeoclimatology, Palaeoecology*, **99**, 9–15.

GRAHN, Y. & PARIS, F. 1992. Age and correlation of the Trombetas Group, Amazonas Basin, Brazil. *Revue de Micropaléontologie*, **35**, 197–209.

GUTIÉRREZ-MARCO, J. C. & ŠTORCH, P. 1998. Graptolite biostratigraphy of the Lower Silurian (Llandovery) shelf deposits of the Western Iberian Cordillera, Spain. *Geological Magazine*, **135**, 71–92.

HAMOUMI, N. 1999. Upper Ordovician glaciation spreading and its sedimentary record in Moroccan North Gondwana margin. *In*: KRAFT, P. & FJÄCKA, O. (eds) *Quo Vadis Ordovician?* Acta Universitatis Carolinae, Geologica, **43**, 111–114.

HATCH, J. R., JACOBSON, S. R., WITZKE, B. J. *ET AL*. 1987. Possible late Middle Ordovician organic carbon isotope excursion: evidence from Ordovician oils and hydrocarbon source rocks, mid-continent and east-central United States. *American Association of Petroleum Geologists, Bulletin*, **71**, 1342–1354.

HAVLÍČEK, V. & MASSA, D. 1973. Brachiopodes de l'Ordovicien Supérieur de Libye occidental: implications stratigraphiques regionales. *Geobios*, **6**, 267–290.

HAYES, J. M., STRAUSS, H. & KAUFMAN, A. J. 1999. The abundance of ^{13}C in marine organic matter and isotopic fractionation in the global biogeochemical cycle of carbon during the past 800 Ma. *Chemical Geology*, **161**, 103–125.

HAYS, P. D. & GROSSMAN, E. L. 1991. Oxygen isotopes in meteoric calcite cements as indicators of continental paleoclimate. *Geology*, **19**, 441–444.

HAYWOOD, A. M., DEKENS, P., RAVELO, A. C. & WILLIAMS, M. 2005. Warmer tropics during the mid-Pliocene? Evidence from alkenone paleothermometry and a fully coupled ocean-atmosphere GCM. *Geochemistry, Geophysics, Geosystems*, **6**, Q03010.

HERRMANN, A. D., PATZKOWSKY, M. E. & POLLARD, D. 2003. Obliquity forcing with 8–12 times preindustrial levels of atmospheric pCO_2 atmospheric CO_2 during the Late Ordovician glaciation. *Geology*, **31**, 485–488.

HERRMANN, A. D., PATZKOWSKY, M. E. & POLLARD, D. 2004*a*. The impact of paleogeography, pCO_2, poleward ocean heat transport and sea level change on global cooling during the Late Ordovician. *Palaeogeography, Palaeoclimatology, Palaeoecology*, **206**, 59–74.

HERRMANN, A. D., HAUPT, B. J., PATZKOWSKY, M. E., SEIDOV, D. & SLINGERLAND, R. L. 2004*b*. Response of Late Ordovician paleoceanography to changes in sea level, continental drift, and atmospheric pCO_2: potential causes for long-term cooling and glaciation. *Palaeogeography, Palaeoclimatology, Palaeoecology*, **210**, 385–401.

HOLLAND, H. D. 1978. *The Chemistry of the Atmosphere and the Ocean.* Wiley Interscience, New York.

HOVIUS, N. 1998. Controls on sediment supply by large rivers. *In*: SHANLEY, K. W. & MCCABE, P. J. (eds) *Relative Role of Eustasy, Climate, and Tectonism in Continental Rocks*. SEPM Special Publication, **59**, 3–16.

HUTT, J. E. 1974. The Llandovery graptolites of the English Lake District. Part 1. *Monograph of the Palaeontographical Society, London*, **128**, 1–56.

JAMES, N. P., BONE, Y. & KYSER, T. K. 1997. Brachiopod δ^{18}O values do reflect ambient oceanography: Lacepede Shelf, southern Australia. *Geology*, **25**, 551–554.

JEPPSSON, L. 1990. An oceanic model for lithological and faunal changes tested on the Silurian record. *Journal of the Geological Society, London*, **147**, 663–674.

JEPPSSON, L. 1997. The anatomy of the Mid–Early Silurian Ireviken Event and a scenario for P–S events. *In*: BRETT, C. E. & BAIRD, G. C. (eds) *Paleontological Events: Stratigraphic, Ecological, and Evolutionary Implications*. Columbia University Press, New York, 451–492.

JEPPSSON, L., ALDRIDGE, R. J. & DORNING, K. J. 1995. Wenlock (Silurian) oceanic episodes and events.

Journal of the Geological Society, London, **152**, 487–498.

JOHNSON, M. E. 1996. Stable cratonic sequences and a standard for Silurian eustasy. *In*: WITZKE, B. J., LUDVIGSON, G. A. & DAY, J. (eds) *Paleozoic Sequence Stratigraphy: Views from the North American Craton.* Geological Society of America Special Paper, **306**, 203–211.

JOHNSON, M. E. 2006. Relationship of Silurian sea-level fluctuations to oceanic episodes and events. *GFF*, **128**, 115–122.

JOHNSON, M. E., KALJO, D. L. & RONG, J.-Y. 1991. Silurian eustasy. *In*: BASSETT, M. G., LANE, P. D. & EDWARDS, D. (eds) *The Murchison Symposium.* Special Papers in Palaeontology, **44**, 145–163.

KALJO, D. & MARTMA, T. 2006. Application of carbon isotope stratigraphy to dating the Baltic Silurian rocks, *GFF*, **128**, 123–129.

KALJO, D., MARTMA, T., MANNIK, P. & VIIRA, V. 2003. Implications of Gondwana glaciations in the Baltic Late Ordovician and Silurian and a carbon isotopic test of environmental cyclicity. *Bulletin de la Société Géologique de France*, **174**, 59–66.

KALJO, D., HINTS, L., HINTS, O., MARTMA, T. & NÕLVAK, J. 1999. Carbon isotope excursions and coeval biotic-environmental changes in the late Caradoc and Ashgill of Estonia. *In*: KRAFT, P. & FJAKA, O. (eds) *Quo Vadis Ordovician?* Acta Universitatis Carolinae, Geologica, **43**, 507–510.

KALJO, D., HINTS, L., MARTMA, T. & NÕLVAK, J. 2001. Carbon isotope stratigraphy in the latest Ordovician of Estonia. *Chemical Geology*, **175**, 49–59.

KALJO, D., HINTS, L., MARTMA, T., NÕLVAK, J. & ORASPÕLD, A. 2004. Late Ordovician carbon isotope trend in Estonia, its significance in stratigraphy and environmental analysis. *Palaeogeography, Palaeoclimatology, Palaeoecology*, **210**, 165–185.

KALJO, D., KIIPLI, T. & MARTMA, T. 1997. Carbon isotope event markers through the Wenlock–Pridoli sequence in Ohesaare (Estonia) and Priekule (Latvia). *Palaeogeography, Palaeoclimatology, Palaeoecology*, **132**, 211–224.

KALJO, D., KIIPLI, T. & MARTMA, T. 1998. Correlation of carbon isotope events and environmental cyclicity in the East Baltic Silurian. *In*: LANDING, E. & JOHNSON, M. E. (eds) *Silurian Cycles: Linkages of Dynamic Stratigraphy with Atmospheric, Oceanic and Tectonic Changes*. New York State Museum Bulletin, **491**, 297–312.

KALJO, D., MARTMA, T. & SAADRE, T. 2007. Post-Hunnebergian Ordovician carbon isotope trend in Baltoscandia, its environmental implications and some similarities with that of Nevada. *Palaeogeography, Palaeoclimatology, Palaeoecology*, in press.

KEGEL, W. 1953. Contribuição para o estudo do. Devoniano da Bacia do Parnaíba. *Boletim da Divisão de Geologia e Mineralogia, Rio de Janeiro*, **141**, 1–48.

KENNEDY, M. J. 1981. The early Palaeozoic Stoneville Formation, northern Newfoundland. *In:* HAMBREY, M. J. & HARLAND, W. B. (eds) *Earth's pre-Pleistocene Glacial Record*. Cambridge University Press, Cambridge, 713–716.

KING, L. M. 1994. Subsidence analysis of eastern Avalonian sequences; implications for Iapetus closure. *Journal of the Geological Society, London*, **151**, 647–657.

KOREN, T. L., POPOV, L. E., DEGTJAREV, K. E., KOVALEVSKY, O. P. & MODZALEVSKAYA, T. L. 2003. Kazakhstan in the Silurian. *In*: LANDING, E. & JOHNSON, M. E. (eds) *Silurian Lands and Seas: Palaeogeography Outside of Laurentia*. New York State Museum, Bulletin, **493**, 323–344.

KUMP, L. R. 2002. Reducing uncertainty about carbon dioxide as a climate driver. *Nature*, **419**, 188–190.

KUMP, L. R. & ARTHUR, M. A. 1999. Interpreting carbon-isotope excursions: carbonates and organic matter. *Chemical Geology*, **161**, 181–198.

KUMP, L. R., ARTHUR, M. A., PATZKOWSKY, M. E., GIBBS, M. T., PINKUS, D. S. & SHEEHAN, P. M. 1999. A weathering hypothesis for glaciation at high atmospheric pCO_2 during the Late Ordovician. *Palaeogeography, Palaeoclimatology, Palaeoecology*, **152**, 173–187.

LE HERON, D. P., SUTCLIFFE, O. E., WHITTINGTON, R. J. & CRAIG, J. 2005. The origins of glacially related soft-sediment deformation structures in Upper Ordovician glaciogenic rocks: implication for ice sheet dynamics. *Palaeogeography, Palaeoclimatology, Palaeoecology*, **218**, 75–103.

LEGGETT, J. K. 1980. British Lower Paleozoic black shales and their palaeo-oceanographic significance. *Journal of the Geological Society, London*, **137**, 139–156.

LEGGETT, J. K. 1987. The Southern Uplands as an accretionary prism; the importance of analogues in reconstructing palaeogeography. *Journal of the Geological Society, London*, **144**, 737–752.

LEGGETT, J. K., MCKERROW, W. S., COCKS, L. R. M. & RICKARDS, R. B. 1981. Periodicity in the early Palaeozoic marine realm. *Journal of the Geological Society*, **138**, 167–176.

LEGGETT, J. K., MCKERROW, W. S., MORRIS, J. H., OLIVER, G. J. H. & PHILLIPS, W. E. A. 1979. The north-western margin of the Iapetus Ocean. *In*: HARRIS, A. L., HOLLAND, C. H. & LEAKE, B. E. (eds) *The Caledonides of the British Isles; reviewed.* Special Publication of the Geological Society, London, **8**, 499–512.

LEGRAND, P. 1969. Description de *Westonia chudeaui* sp. nov. Brachiopode inarticulé de l'Adrar mauritanien (Sahara occidental). *Bulletin de la Société Géologique de France*, **11**, 251–256.

LEGRAND, P. 1970. Les couches à *Diplograptus* du Tassili de Tarit (Ahmet, Sahara algérien). *Bulletin de la Société d'Histoire Naturelle de Afrique du Nord*, **60**, 3–58.

LEGRAND, P. 1985. Lower Palaeozoic rocks of Algeria. *In*: HOLLAND, C. H. (ed.) *Lower Palaeozoic of North-Western and West-Central Africa. Lower Palaeozoic Rocks of the World*, **4**, 5–89, John Wiley & Sons, Chichester.

LOCKLAIR, R. E. & LERMANN, A. 2005. A model of Phanerozoic cycles of carbon and calcium in the global ocean: Evaluation and constraints on ocean chemistry and input fluxes. *Chemical Geology*, **217**, 113–126.

LOWENSTAM, H. A. 1961, Mineralogy, $^{18}O/^{13}C$ ratios, and strontium and magnesium contents of recent and fossil brachiopods and their bearing on the history of oceans. *Journal of Geology*, **69**, 241–260.

Loydell, D. K. 1994. Early Telychian changes in graptoloid diversity and sea level. *Geological Journal*, **29**, 355–368.

Loydell, D. K. 1998. Early Silurian sea-level changes. *Geological Magazine*, **135**, 447–471.

Loydell, D. K. & Nestor, V. 2005. Integrated graptolite and chitinozoan biostratigraphy of the upper Telychian (Llandovery, Silurian) of the Ventspils D-3 core, Latvia. *Geological Magazine*, **142**, 369–376.

Loydell, D. K., Kaljo, D. & Männik, P. 1998. Integrated biostratigraphy of the lower Silurian of the Ohesaare core, Saaremaa, Estonia. *Geological Magazine*, **135**, 769–783.

Loydell, D. K., Männik, P. & Nestor, V. 2003. Integrated biostratigraphy of the lower Silurian of the Aizpute-41 core, Latvia. *Geological Magazine*, **140**, 205–229.

Ludvigson, G. A., Witzke, B. J., Gonzalez, L. A., Carpenter, S. J., Schneider, C. L. & Hasiuk, F. H. 2004. Late Ordovician (Turinian–Chatfieldian) carbon isotope excursions and their paleoceanographic significance. *Palaeogeography, Palaeoclimatology, Palaeoecology*, **210**, 187–214.

Lüning, S., Craig, J., Loydell, D. K., Storch, P. & Fitches, B. 2000. Lower Silurian 'hot shales' in North Africa and Arabia: regional distribution and depositional model. *Earth Science Reviews*, **49**, 21–200.

Lüning, S., Loydell, D. K., Štorch, P., Shahin, Y. & Craig, J. 2006. Origin, sequence stratigraphy and depositional environment of an upper Ordovician (Hirnantian) deglacial black shale, Jordan – Discussion. *Palaeogeography, Palaeoclimatology, Palaeoecology*, **230**, 352–355.

Lüning, S., Shahin, Y. M., Loydell, D. K., Al-Rabi, H. T., Masri, A., Tarawneh, B. & Kolonic, S. 2005. Anatomy of a world-class source rock: distribution and depositional model of Silurian organic-rich shales in Jordan and implications for hydrocarbon potential. *AAPG Bulletin*, **89**, 1397–1427.

Maack, R. 1957. Über Vereisungsperioden und Vereisungsspuren in Brasilien. *Geologische Rundschau*, **45**, 547–595.

Mabillard, J. E. & Aldridge, R. J. 1985. Microfossil distribution across the base of the Wenlock Series in the type area. *Palaeontology*, **28**, 89–100.

Männil, R. & Meidla, T. 1994. The Ordovician System of the East European Platform (Estonia, Latvia, Lithuania, Belorussia, parts of Russia, Ukraine and Moldova). *In*: Webby, B. D., Ross, R. J. & Zhen, Y. Y. (eds) *The Ordovician System of the East European Platform and Tuva (southeastern Russia).* IUGS Publication, **28**, 1–52.

Marshall, J. D., Brenchley, P. J., Mason, P., Wolff, G. A., Astini, R. A., Hints, L. & Meidla, T. 1997. Global carbon isotopic events associated with mass extinction and glaciation in the late Ordovician. *Palaeogeography, Palaeoclimatology, Palaeoecology*, **132**, 195–210.

Martin, R. E. 1995. Cyclic and secular variation in microfossil biomineralization – clues to the biogeochemical evolution of Phanerozoic oceans. *Global and Planetary Change*, **11**, 1–23.

McCann, A. M. & Kennedy, M. J. 1974. A probable glacio-marine deposit of Late Ordovician–Early Silurian age from the north central Newfoundland Appalachian Belt. *Geological Magazine*, **111**, 549–564.

McClure, H. A. 1978. Early Palaeozoic glaciation in Arabia. *Palaeogeography, Palaeoclimatology, Palaeoecology*, **25**, 315–326.

McKerrow, W. S., Mac Niocaill, C. & Dewey, J. F. 2000. The Caledonian Orogeny redefined. *Journal of the Geological Society, London*, **157**, 1149–1154.

Melchin, M. J. 1989. Llandovery graptolite biostratigraphy and paleobiogeography, Cape Phillips Formation, Canadian Arctic Islands. *Canadian Journal of Earth Sciences*, **26**, 1726–1746.

Melchin, M. J. & Holmden, C. 2006. Carbon isotope chemostratigraphy in Arctic Canada: Sea-level forcing of carbonate platform weathering and implications for Hirnantian global correlation. *Palaeogeography, Palaeoclimatology, Palaeoecology*, **234**, 186–200.

Melchin, M. J., Cooper, R. A. & Sadler, P. M. 2004. The Silurian Period. *In*: Gradstein, F. M., Ogg, J. G. & Smith, A. G. (eds) *A Geologic Time Scale 2004.* Cambridge University Press, Cambridge, 165–187.

Merino, D. 1991. Primer registro de conodontos siluricos en Bolivia. *Revisita Tecnica de YPFB*, **12**, 271–274.

Meybeck, M. 1982. Carbon, nitrogen, and phosphorus transport by world rivers. *American Journal of Science*, **282**, 401–450.

Miller, M. A. & Melvin, J. 2005. Significant new biostratigraphic horizons in the Qusaiba member of the Silurian Qalibah formation of central Saudi Arabia, and their sedimentologic expression in a sequence stratigraphic context. *GeoArabia*, **10**, 49–92.

Montañez, I. P. 2002. Biological skeletal carbonate records changes in major-ion chemistry of paleo-oceans. *PNAS*, **99**, 15852–15854.

Mu, E.-Z. 1988. The Ordovician–Silurian boundary in China. *Bulletin of the British Museum (Natural History)*, **43**, 117–131.

Mullins, G. L. & Aldridge, R. J. 2004. Chitinozoan biostratigraphy of the basal Wenlock Series (Silurian) global stratotype section and point. *Palaeontology*, **47**, 745–773.

Munnecke, A., Samtleben, C. & Bickert, T. 2003. The Ireviken event in the Lower Silurian of Gotland, Sweden – relation to similar Palaeozoic and Proterozoic events. *Palaeogeography, Palaeoclimatology, Palaeoecology*, **195**, 99–124.

Nielsen, A. T. 2003*a*. Ordovician sea level changes: a Baltoscandinavian perspective. *In*: Webby, B. D., Paris, F., Droser, M. & Percival, I. G. (eds) *The Great Ordovician Biodiversification Event.* Columbia University Press, New York, 84–93.

Nielsen, A. T. 2003*b*. Late Ordovician sea level changes: evidence of Caradoc glaciations? *Geophysical Research Abstracts, European Geosciences Union*, **5**.

Nõlvak, J., Hints, O. & Männik, P. 2006. Ordovician timescale in Estonia: recent developments. *Proceedings of the Estonian Academy of Sciences, Geology*, **55**, 95–108.

Oldroyd, D. R. 1990. *The Highland Controversy: Constructing Geological Knowledge through Fieldwork in*

Nineteenth-Century Britain. Science and Its Conceptual Foundations series. Chicago University Press, Chicago.

ORR, P. J. 2001. Bathymetric Indicators. *In*: BRIGGS, D. E. G. & CROWTHER, P. R. (eds) *Palaeobiology II*. Blackwell Science, Oxford, 479–482.

PANCOST, R. D., FREEMAN, K. H., PATZKOWSKY, M. E., WAVREK, D. & COLLISTER, J. W. 1998. Molecular indicators of redox and marine photoautotroph composition in the late Middle Ordovician of Iowa, USA. *Organic Geochemistry*, **29**, 1649–1662.

PARRISH, J. T. 1982. Upwelling and petroleum source beds, with reference to the Palaeozoic. *AAPG Bulletin*, **66**, 750–774.

PATZKOWSKY, M. E., SLUPIK, L. M., ARTHUR, M. A., PANCOST, R. D. & FREEMAN, K. H. 1997. Late Middle Ordovician environmental change and extinction: harbinger of the Late Ordovician or continuation of Cambrian patterns? *Geology*, **25**, 911–914.

PHILLIPOT, A. & ROBARDET, M. 1971. Nouvelles donnees sur les formations siluriennes de Domfront (Orne). *Bulletin de la Société Géologique et Mineralogique de Bretagne, Serie C*, **3**, 41–47.

PICKERILL, R. K., PAJARI, G. E. & CURRIE, K. L. 1979. Evidence of Caradocian glaciation in the Davidsville Group of north-eastern Newfoundland. *Current Research, Part C, Papers of the Canadian Geological Survey*, **79**, 67–72.

PORĘBSKA, E. & SAWŁOWICZ, Z. 1997. Palaeoceanographic linkage of geochemical and graptolite events across the Silurian–Devonian boundary in Bardzkie Mountains (Southwest Poland). *Palaeogeography, Palaeoclimatology, Palaeoecology*, **132**, 343–354.

PRATT, W. T., WOODHALL, D. G. & HOWELLS, M. F. 1995. Geology of the country around Cadair Idris. Memoir for 1:50,000 Geological Sheet 149 (England and Wales). London, HMSO.

RAHMSTORF, S. 2002. Ocean circulation and climate during the past 120,000 years, *Nature*, **419**, 207–214.

RAYMO, M. E. 1991. Geochemical evidence supporting T.C. Chamberlin's theory of glaciation. *Geology*, **19**, 344–347.

RICKARDS, R. B. 1970. The Llandovery (Silurian) graptolites of the Howgill Fells, Northern England. *Palaeontographical Society Monographs*, **123**, 1–108.

RICKARDS, R. B. & WOODCOCK, N. H. 2005. Stratigraphical revision of the Windermere Supergroup (Late Ordovician–Silurian) in the southern Howgill Fells, NW England. *Proceedings of the Yorkshire Geological Society*, **55**, 263–285.

RIDGWELL, A. 2005. A Mid Mesozoic Revolution in the regulation of ocean chemistry. *Marine Geology*, **217**, 339–357.

ROBARDET, M., HENRY, J. L., NION, J., PARIS, F. & PILLET, J. 1972. La Formation du Pont-de-Caer (Caradocien) dans les synclinaux de Domfront et de Sees (Normandie). *Société Géologique du Nord, Annales*, **92**, 117–137.

ROCHA-CAMPOS, A. C. 1981. Early Palaeozoic Iapo Formation of Paraná, Brazil. *In*: HAMBREY, M. J. & HARLAND, W. B. (eds) *Earth's pre-Pleistocene Glacial Record*. Cambridge University Press, Cambridge, 908–909.

ROHLING, E. J. & GIESKES, W. W. C. 1989. Late Quaternary changes in Mediterranean Intermediate Water density and formation rate. *Paleoceanography*, **4**, 531–545.

ROHLING, E. J. 1994. Review and new aspects concerning the formation of Mediterranean sapropels, *Marine Geology*, **122**, 1–28.

RONG, J.-Y., BOUCOT, A. J., SU, Y.-Z. & STRUSZ, D. L. 1995. Biogeographical analysis of Late Silurian brachiopod faunas, chiefly from Asia and Australia. *Senckenberg Lethaea*, **28**, 39–60.

RONOV, A. B., KHAIN, V. E., BALUKHOVSKY, A. N. & SESLAVINSKY, K. B. 1980. Quantitative analysis of Phanerozoic sedimentation. *Sedimentary Geology*, **25**, 311–325.

ROSS, C. A. & ROSS, J. R. P. 1995. North American Ordovician depositional sequences and correlations. *In*: COOPER, J. D. & FINNEY, S. C. (eds) *Ordovician Odyssey. SEPM, Pacific Section*, Fullerton California, 309–313.

ROSS, C. A. & ROSS, R. P. 1996. Silurian sea-level fluctuations. *In*: WITZKE, B. J., LUDVIGSON, G. A. & DAY, J. (eds) *Paleozoic Sequence Stratigraphy: Views from the North American Craton*. Geological Society of America, Special Paper, **306**, 187–192.

ROTHMAN, D. H., HAYES, J. M. & SUMMONS, R. E. (2003) Dynamics of the Neoproterozoic carbon cycle. *Proceedings of the National Academy of Science*, **100**, 8124–8129.

ROYER, D. L. 2006. CO_2-forced climate thresholds during the Phanerozoic. *Geochimica et Cosmochimica Acta*, **70**, 566–567.

ROYER, D. L., BERNER, R. A., MONTAÑEZ, I. P., TABOR, N. J. & BEERLING, D. J. 2004. CO_2 as a primary driver of Phanerozoic climate. *GSA Today*, **14**, 4–10.

RUDWICK, M. J. S. 1985. *The great Devonian controversy: The shaping of scientific knowledge among gentlemanly specialists*. Science and its conceptual foundations series. Chicago University Press, Chicago.

RUST, I. C. 1981. Early Palaeozoic Pakhuis Tillite, South Africa. *In*: HAMBREY, M. J. & HARLAND, W. B. (eds) *Earth's pre-Pleistocene Glacial Record*. Cambridge University Press, Cambridge, 113–117.

SALTZMAN, M. R. 2005. Phosphorus, nitrogen, and the redox evolution of the Paleozoic oceans. *Geology*, **33**, 573–576.

SALTZMAN, M. R. & YOUNG, S. A. 2005. A long-lived glaciation in the Late Ordovician? Isotopic and sequence stratigraphic evidence from western Laurentia. *Geology*, **33**, 109–112.

SAMTLEBEN, C., MUNNECKE, A., BICKERT, T. & PÄTZOLD, J. 2001. Shell succession, assemblage and species dependent effects on the C/O-isotopic composition of brachiopods: examples from the Silurian of Gotland. *Chemical Geology*, **175**, 61–107.

SAMTLEBEN, C., MUNNECKE, A., BICKERT, T. & PÄTZOLD, J. 1996. The Silurian of Gotland (Sweden): Facies interpretation based on stable isotopes in brachiopod shells. *Geologische Rundschau*, **85**, 278–292.

SCHENCK, P. E. 1972. Possible Late Ordovician glaciation of Nova Scotia. *Canadian Journal of Earth Science*, **9**, 95–107.

SCHENCK, P. E. & LANE, T. E. 1981. Early Paleozoic tillite of Nova Scotia, Canada. *In*: HAMBREY, M. J. & HARLAND, W. B. (eds) *Earth's pre-Pleistocene Glacial Record*. Cambridge University Press, Cambridge, 707–710.

SCHOFIELD, D. I., DAVIES, J. R, WATERS, R. A., WILBY, P. R., WILLIAMS, M. & WILSON, D. 2004. Geology of the Builth Wells district – a brief explanation of the geological map. Sheet explanation of the British Geological Survey. 1:50000 sheet 196 Builth Wells (England & Wales). Keyworth, Nottingham, British Geological Survey.

SCOTESE, C. R. & MCKERROW, W. S. 1991. Ordovician plate tectonic reconstructions. *Canadian Geological Survey Paper*, **90–99**, 271–282.

SCRIVNER, A. E., VANCE, D. & ROHLING, E. J. 2004. New neodymium isotope data quantify Nile involvement in Mediterranean anoxic episodes. *Geology*, **32**, 565–568.

SECORD, J. A. 1986. *Controversy in Victorian geology: the Cambrian–Silurian dispute*. Princeton University Press, Princeton.

SHACKLETON, N. J. 2000. The 100,000-year ice-age cycle identified and found to lag temperature, carbon dioxide, and orbital eccentricity. *Science*, **289**, 1897–1902.

SHAVIV, N. J. 2002. Cosmic ray diffusion from the galactic spiral arms, iron meteorites, and a possible climatic connection. *Physical Review Letters*, **89**, art. no. 051102.

SHAVIV, N. J. & VEIZER, J. 2003. Celestial driver of Phanerozoic climate?, *GSA Today*, **13**, 4–10.

SHIELDS, G. A., CARDEN, G. A. F., VEIZER, J., MEIDLA, T., RONG, J.-Y. & LI, R.-Y. 2003. Sr, C and O isotope geochemistry of Ordovician brachiopods: a major isotopic event around the Middle–Late Ordovician transition. *Geochimica et Cosmochimica Acta*, **67**, 2005–2025.

SHUSTER, D. L., EHLERS, T. A., RUSMOREN, M. E. & FARLEY, K. A. 2005. Rapid glacial erosion at 1.8 Ma revealed by $^4He/^3He$ thermochronometry. *Science*, **310**, 1668–1670.

SIEGENTHALER, U., STOCKER, T., MONNIN, E. *ET AL.* 2005. Stable carbon cycle-climate relationship during the late Pleistocene. *Science*, **310**, 1313–1317.

SKEVINGTON, D. 1974. Controls influencing the composition and distribution of Ordovician graptolite provinces. *In*: RICKARDS, R. B., JACKSON, D. E. & HUGHES, C. P. (eds) *Graptolite Studies in Honour of O. M. B. Bulman.* Special Papers in Palaeontology, **13**, 59–73.

SMITH, A. G. & PICKERING, K. T. 2003. Oceanic gateways as a critical factor to initiate icehouse Earth. *Journal of the Geological Society*, **160**, 337–340.

ŠTORCH, P. 1986. Ordovician–Silurian boundary in the Prague Basin (Barrandian area, Bohemia). *Sborník Geologických věd, Geologie*, **41**, 69–103.

ŠTORCH, P. 1994. Graptolite biostratigraphy of the Lower Silurian (Llandovery and Wenlock) of Bohemia. *Geological Journal*, **29**, 137–165.

ŠTORCH, P. & MERGL, M. 1989. Králodvor/Kosov boundary and the late Ordovician environmental changes in the Prague Basin (Barrandian area, Bohemia). *Sborník Geologických Věd, Geologie*, **44**, 117–153.

STRACHAN, R. A. 2000. Mid-Ordovician to Silurian sedimentation and tectonics on the northern active margin of Iapetus. *In*: WOODCOCK, N. H. & STRACHAN, R. A. (eds) *Geological History of Britain Ireland*. Blackwell, Oxford, 107–123.

SUÁREZ-SORUCO, R. 1995. Comentarios sobre la edad de la Formacion Cancañiri. *Revista Tecnica de Yacamientos Petroliferos Fisicales Bolivianos*, **16**, 51–54.

SUTCLIFFE, O. E., DOWDESWELL, J. A., WHITTINGTON, R. J., THERON, J. N. & CRAIG, J. 2000. Calibrating the Late Ordovician glaciation and mass extinction by the eccentricity of Earth's orbit. *Geology*, **28**, 967–970.

SUTCLIFFE, O. E., HARPER, D. A. T., SALEM, A. A., WHITTINGTON, R. J. & CRAIG, J. 2001. The development of an atypical *Hirnantia* brachiopod fauna and the onset of glaciation in the late Ordovician of Gondwana. *Transactions of the Royal Society of Edinburgh, Earth Sciences*, **92**, 1–14.

THONG-DZUY, T., BOUCOT, A. J., RONG, J.-Y. & FANF, Z.-J. 2001. Late Silurian marine shelly fauna of Central and Northern Vietnam. *Geobios*, **34**, 315–338.

TOBIN, K. J., BERGSTRÖM, S. M. & DE LA GARZA, P. 2005. A mid-Caradocian (453 Ma) drawdown in atmospheric pCO_2 atmospheric CO_2 without ice sheet development? *Palaeogeography, Palaeoclimatology, Palaeoecology*, **226**, 187–204.

TOGHILL, P. 1968. The graptolite assemblages and zones of the Birkhill Shales (Lower Silurian) at Dobb's Linn. *Palaeontology*, **11**, 654–678.

TORSVIK, T. H. 1998. Palaeozoic palaeogeography: A North Atlantic viewpoint. *GFF*, **120**, 109–118.

TUCKER, M. E. & REID, P. C. 1973. The sedimentology and context of late Ordovician glacial marine sediments from Sierra Leone, West Africa. *Palaeogeography, Palaeoclimatology, Palaeoecology*, **13**, 289–307.

UNDERWOOD, C. J. 1992. Graptolite Preservation and Deformation. *Palaios*, **7**, 178–186.

UNDERWOOD, C. J., CROWLEY, S. F., MARSHALL, J. D. & BRENCHLEY, P. J. 1997. High resolution carbon isotope stratigraphy of the basal Silurian stratotype (Dob's Linn, Scotland) and its global correlation. *Journal of the Geological Society, London*, **154**, 709–718.

UNDERWOOD, C. J., DEYNOUX, M. & GHIENNE, J.-F. 1998. High Palaeolatitude (Hodh, Mauritania) recovery of graptolite fauna after the Hirnantian (end Ordovician) extinction event. *Palaeogeography, Palaeoclimatology, Palaeoecology*, **142**, 91–105.

VEIZER, J., BRUCKSCHEN, P. & PAWELLEK, F. *ET AL.* 1997. Oxygen isotope evolution of Phanerozoic seawater. *Palaeogeography, Palaeoclimatology, Palaeoecology*, **132**, 159–172.

VEIZER, J., GODDERIS, Y. & FRANÇOIS, L. M. 2000. Evidence for decoupling of atmospheric CO_2 and global climate during the Phanerozoic eon. *Nature*, **408**, 698–701.

VELBEL, M. A. 1993. Temperature dependence of silicate weathering in nature: How strong a negative feedback on long-term accumulation of atmospheric CO_2 and global greenhouse warming? *Geology*, **21**, 1059–1062.

VERNIERS, J. & VANDENBROUCKE, T. R. A. 2006. Chitinozoan biostratigraphy in the Dob's Linn Ordovician–Silurian GSSP, Southern Uplands, Scotland. *GFF*, **128**, 195–202.

WALKER, L. J., WILKINSON, B. H. & IVANY, L. C. 2002. Continental drift and Phanerozoic carbonate accumulation in shallow-shelf and deep-marine settings. *Journal of Geology*, **110**, 75–87.

WHITE, D. E., BARRON, H. F., BARNES, R. P. & LINTERN, B. C. 1991. Biostratigraphy of late Llandovery (Telychian) and Wenlock turbiditic sequences in the SW Southern Uplands, Scotland. *Transactions of the Royal Society of Edinburgh, Earth Sciences*, **82**, 297–322.

WIGNALL, P. B. 1991. Model for transgressive black shales? *Geology*, **19**, 167–170.

WIGNALL, P. B. 1994. *Black Shales*. Clarendon Press, Oxford.

WIGNALL, P. B. & MAYNARD, J. R. 1993. The sequence stratigraphy of transgressive black shales. *In*: KATZ, B. J. & PRATT, L. (eds) *Source Rocks within a Sequence Stratigraphic Framework*. American Association of Petroleum Geologists Studies in Geology, **37**, 35–47.

WILLIAMS, M., DAVIES, J. R., WATERS, R. A., RUSHTON, A. W. A. & WILBY, P. R. 2003. Stratigraphical and palaeoecological importance of Caradoc (Upper Ordovician) graptolites from the Cardigan area, southwest Wales. *Geological Magazine*, **140**, 549–571.

WILLIAMS, M., RUSHTON, A. W. A., WOOD, B., FLOYD, J. D., SMITH, R. & WHEATLEY, C. 2004. A revised graptolite biostratigraphy for the lower Caradoc (Upper Ordovician) of southern Scotland. *Scottish Journal of Geology*, **40**, 97–114.

WILLIAMS, S. H. 1982. The Late Ordovician fauna of the *anceps* bands at Dob's Linn, southern Scotland. *Geologica et Palaeontologica*, **16**, 29–56.

WOODCOCK, N. H. 1990. Sequence stratigraphy of the Palaeozoic Welsh Basin. *Journal of the Geological Society, London*, **147**, 537–547.

WOODCOCK, N. H. 2000. Late Ordovician to Silurian evolution of Eastern Avalonia during convergence with Laurentia. *In*: WOODCOCK, N. H. & STRACHAN, R. A. (eds) *Geological History of Britain and Ireland*. Blackwell, Oxford.

WOODCOCK, N. H., BUTLER, A. J., DAVIES, J. R. & WATERS, R. A. 1996. Sequence stratigraphical analysis of late Ordovician and early Silurian depositional systems in the Welsh Basin: a critical assessment. *In*: HESSELBO, S. P. & PARKINSON, D. N. (eds) *Sequence Stratigraphy in British Geology*. Special Publication of the Geological Society of London, **103**, 197–208.

YAPP, C. J. & POTHS, H. 1992. Ancient atmospheric CO_2 pressures inferred from natural goethites. *Nature*, **355**, 342–344.

YOLKIN, E. A., SENNIKOV, N. V., BAKHAREV, N. K., IXOKH, N. G. & YAZIKOV, A. YU. 1997. Periodicity of deposition in the Silurian and relationships of global geological events in the middle Paleozoic of the southwestern margin of the Siberian continent. *Geologiya i Geofizika*, **38**, 596–607.

YOUNG, G. M. 1981. Early Palaeozoic tillites of the northern Arabian Peninsula. *In*: HAMBREY, M. J. & HARLAND, W. B. (eds) *Earth's Pre-Pleistocene Glacial Record*. Cambridge University Press, Cambridge, 338–340.

YOUNG, S. A., SALTZMAN, M. R. & BERGSTROM, S. A. 2005. Upper Ordovician (Mohawkian) carbon isotope stratigraphy in Eastern and Central North America: regional expression of a perturbation of the global carbon cycle. *Palaeogeography, Palaeoceanography, Palaeoclimatology*, **222**, 53–76.

ZACHOS, J., PAGANI, M., SLOAN, L., THOMAS, E. & BILLUPS, K. 2001. Trends, rhythms, and aberrations in global climate 65 Ma to present. *Science*, **292**, 686–693.

ZALASIEWICZ, J. A. 2001. Graptolites as constraints on models of sedimentation across Iapetus: a review. *Proceedings of the Geologists Association*, **112**, 237–251.

ZALASIEWICZ, J. A. & WILLIAMS, M. 1999. Graptolite biozonation of the Wenlock Series (Silurian) of the Builth Wells district, central Wales. *Geological Magazine*, **136**, 263–283.

ZALASIEWICZ, J. A., RUSHTON, A. W. A. & OWEN, A. W. 1995. Late Caradoc graptolitic faunal gradients across the Iapetus Ocean. *Geological Magazine*, **132**, 611–617.

ZALASIEWICZ, J., WILLIAMS, M., MILLER, M., PAGE, A. & BLACKETT, E. 2007. Early Silurian (Llandovery) graptolites from central Saudi Arabia: first documented record of Telychian faunas from the Arabian Peninsula. *GeoArabia*, **12**, in press.

ZHANG, S., BARNES, C. R. & JOWETT, D. M. S. 2006. The paradox of the global standard Late Ordovician–Early Silurian sea level curve: Evidence from conodont community analysis from both Canadian Arctic and Appalachian margins. *Palaeogeography, Palaeoclimatology, Palaeoecology*, **236**, 246–271.